
Cathodes for Li-Ion Batteries: Challenges and Prospects

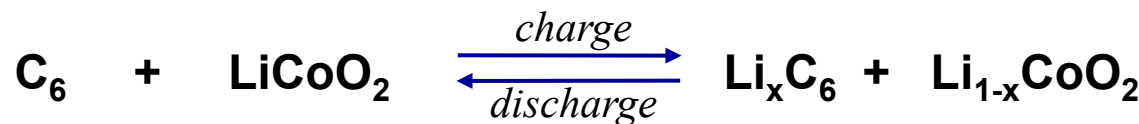
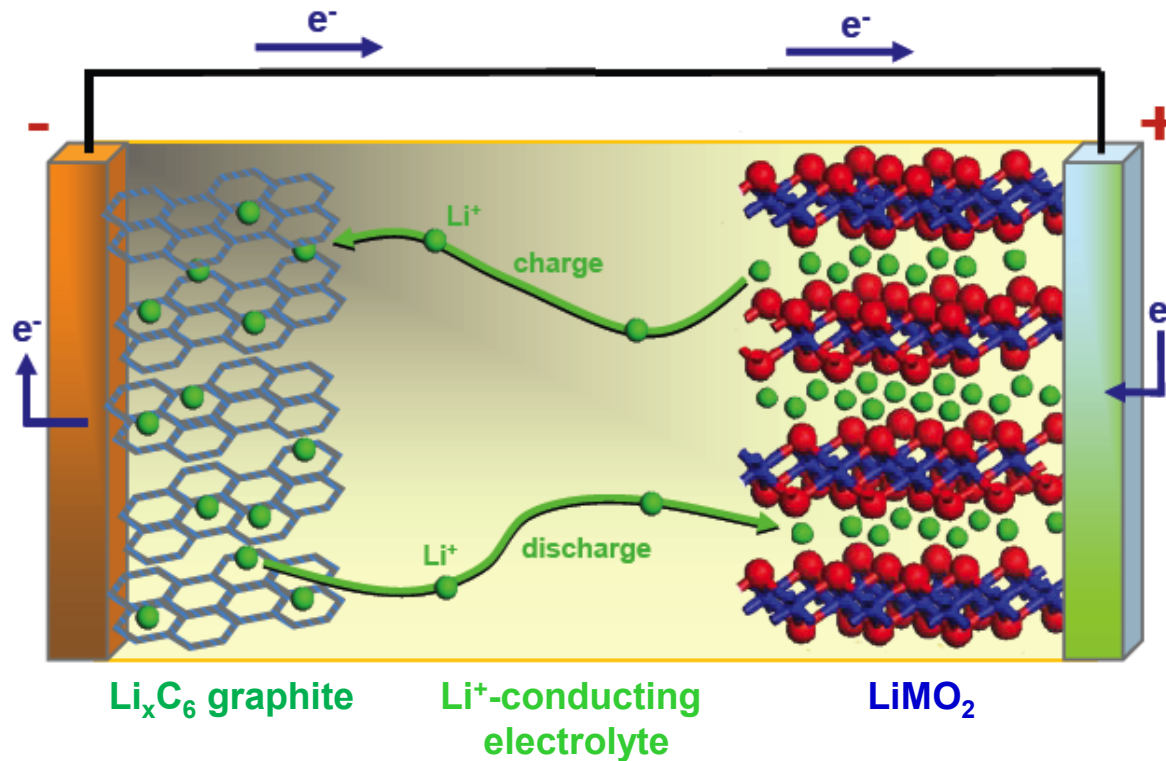
Artem Abakumov

Center for Electrochemical Energy Storage, Skoltech

Outline

1. Li-ion batteries
2. Cathode materials: key parameters and structures
3. Layered Li-rich cathodes: lattice oxygen redox
4. Layered Li-rich cathodes: cation migration and voltage fade
5. Polyanion cathodes: adjusting the redox potential
6. Conclusions

Li-ion batteries



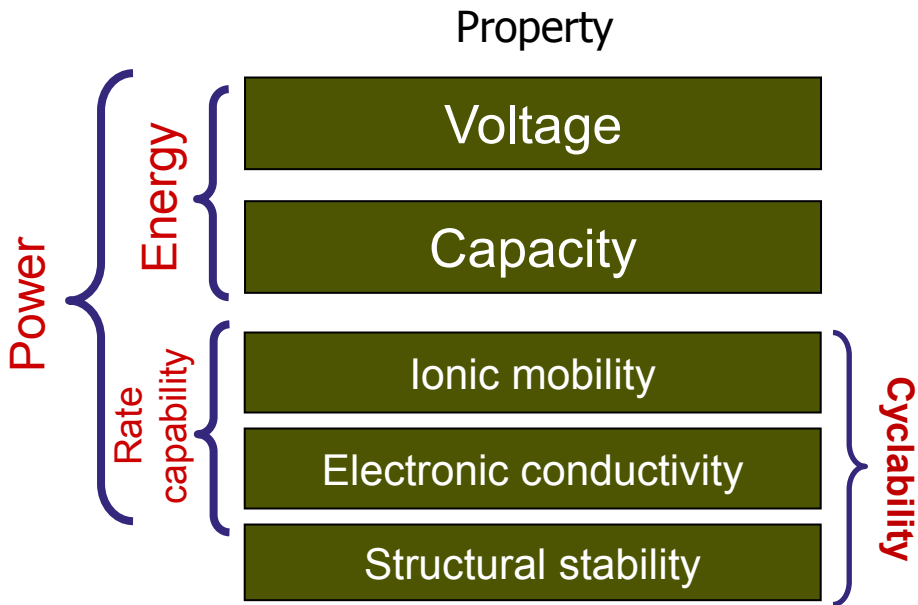
Voltage 3.6 V, $x \approx 0.5\text{-}0.6$ e⁻

Electrolyte:

Li-salt - LiPF₆, LiBF₄ (LiClO₄, LiAsF₆), LiCF₃SO₃

Solvent – ethylene carbonate (CH₂O)₂C, dimethyl carbonate (CH₃O)₂CO

Cathode materials: key properties



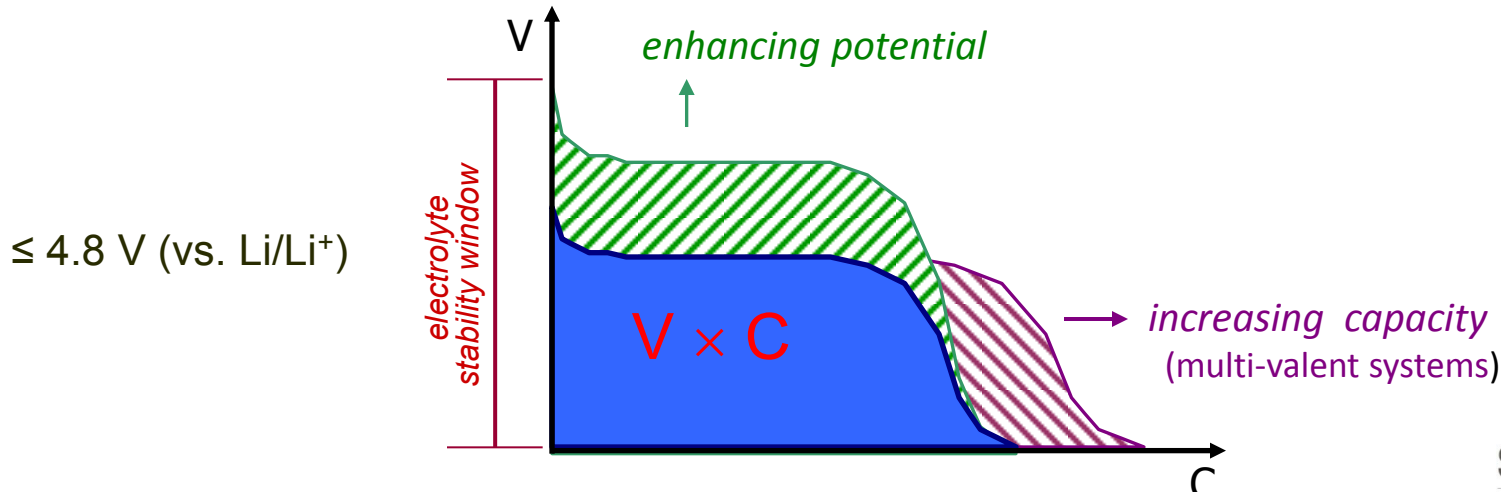
$M^{n+}/M^{(n+1)+}$ redox potential

$$C_T (\text{A h g}^{-1}) = \frac{26.8 \times \Delta n}{M}$$

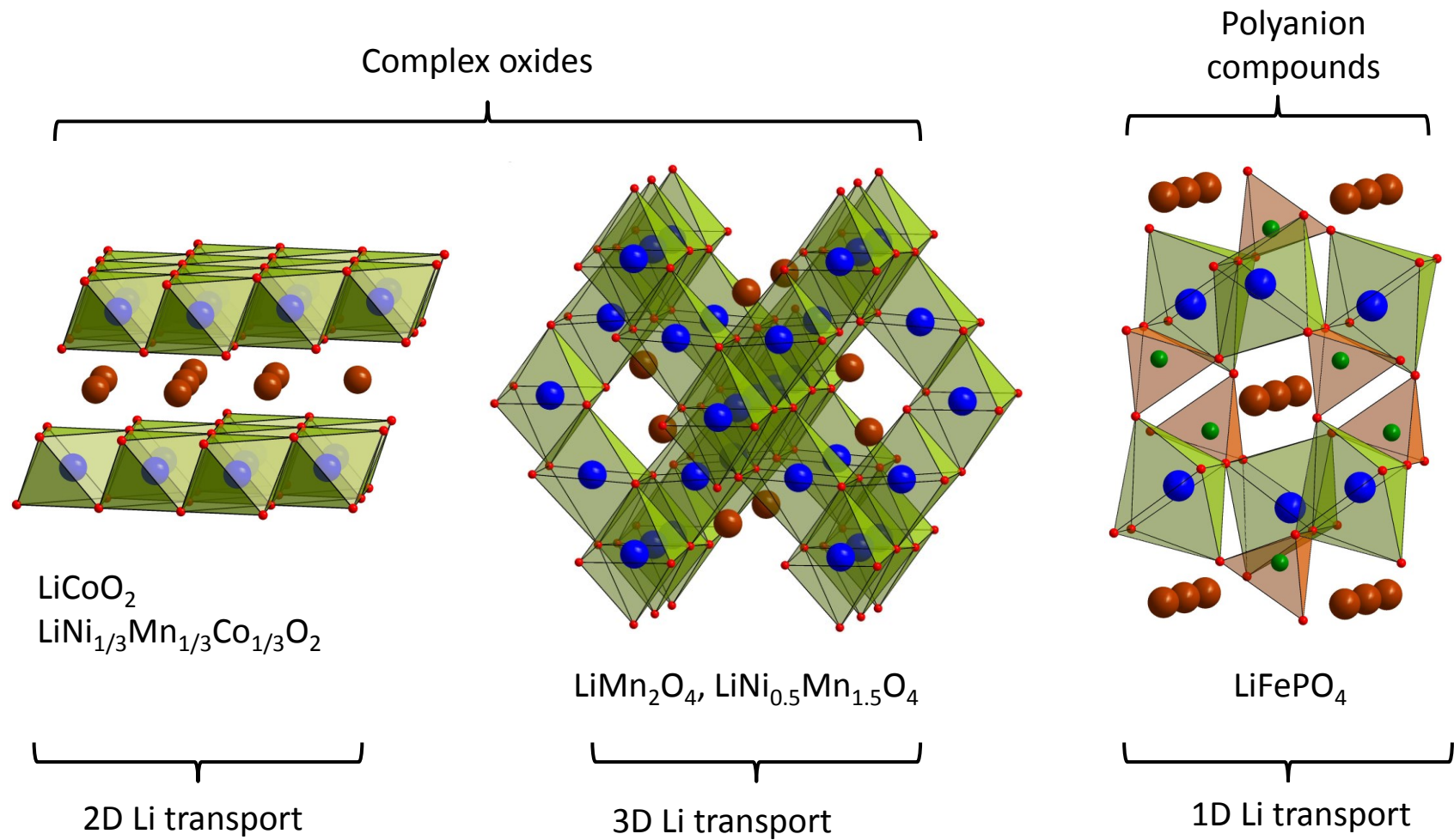
number of e^- or Li^+

Molecular weight (g)

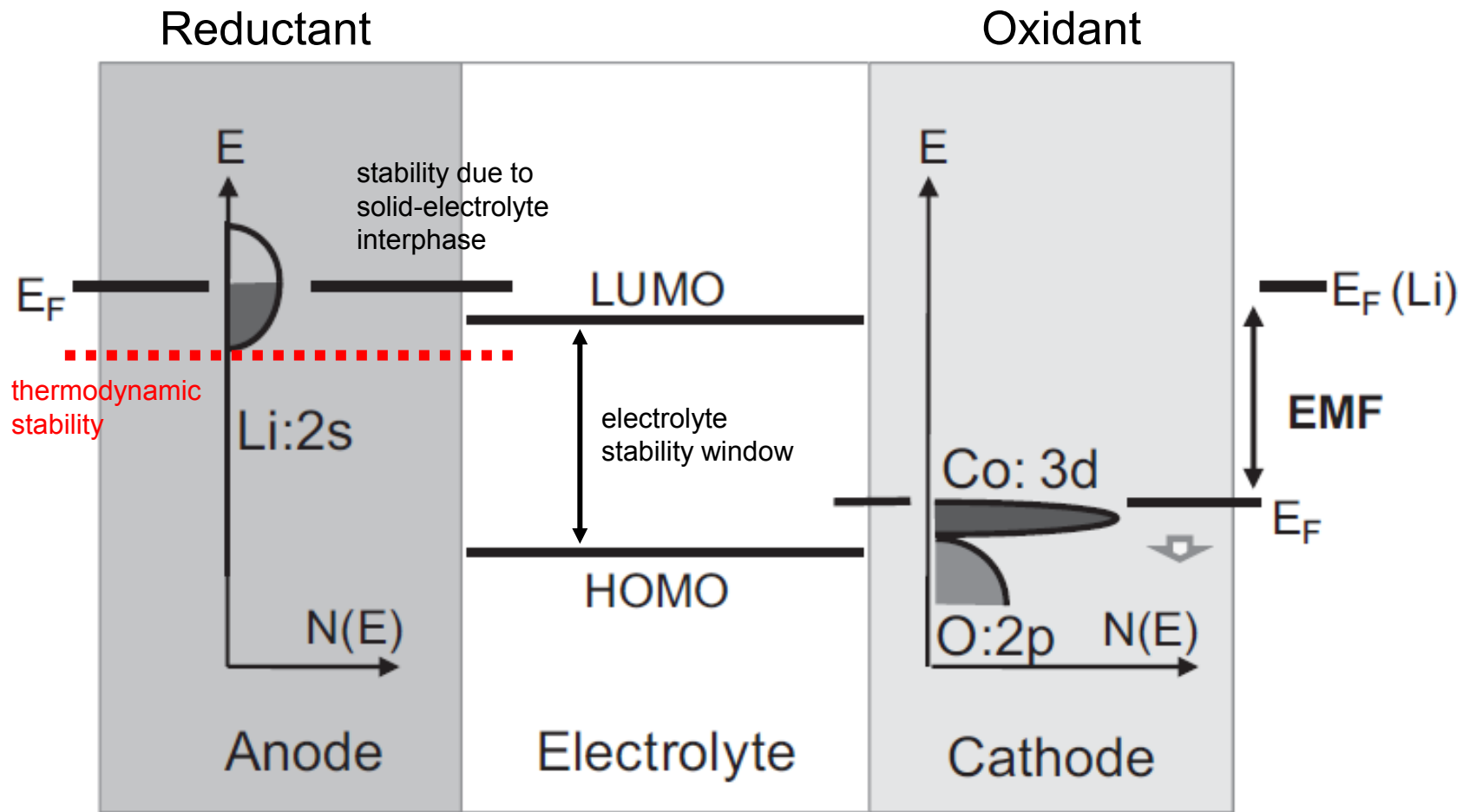
$$\text{Energy} = \text{Voltage} \times \text{Capacity}$$



Cathode materials



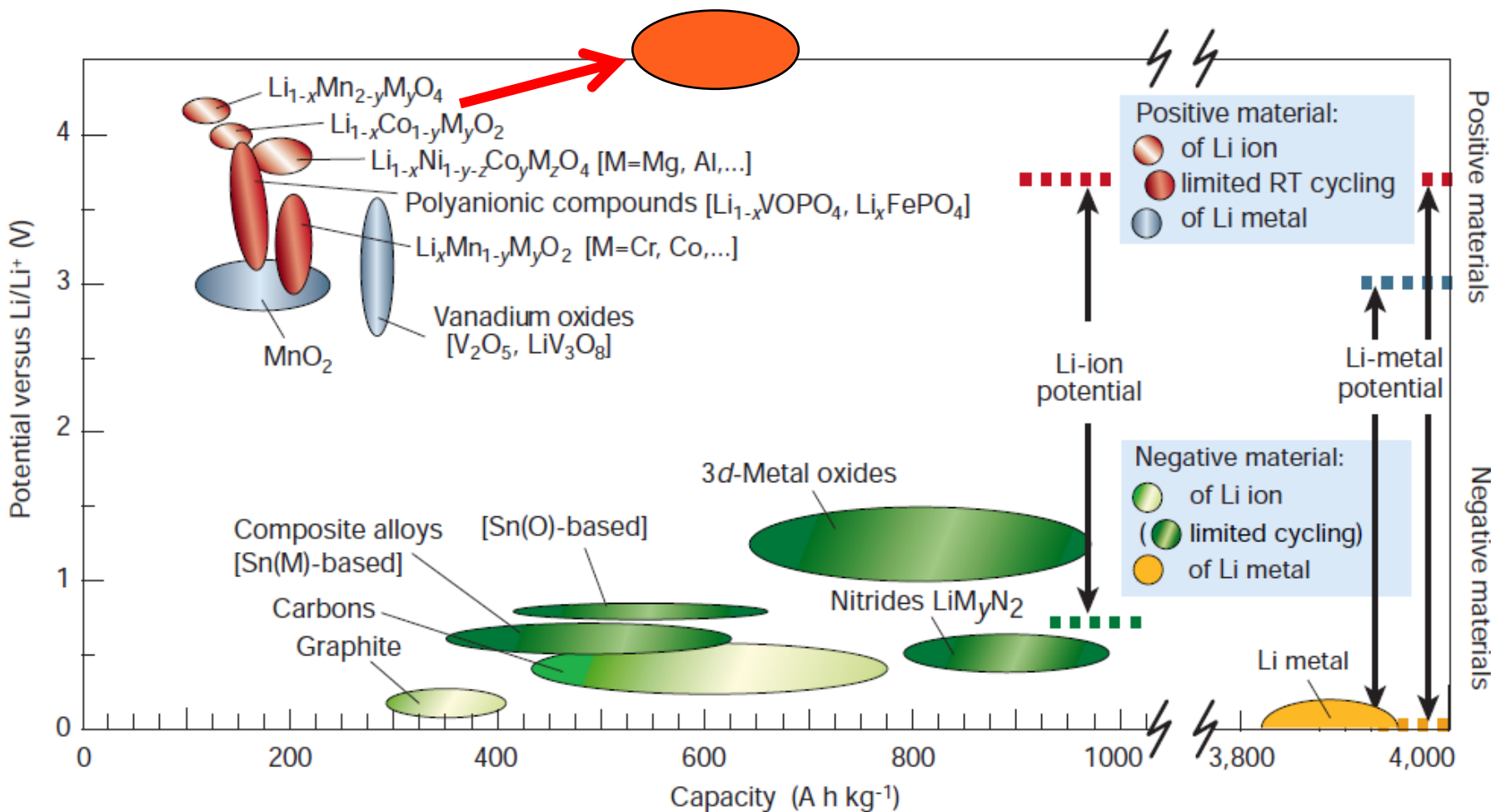
Li-ion battery energy diagram



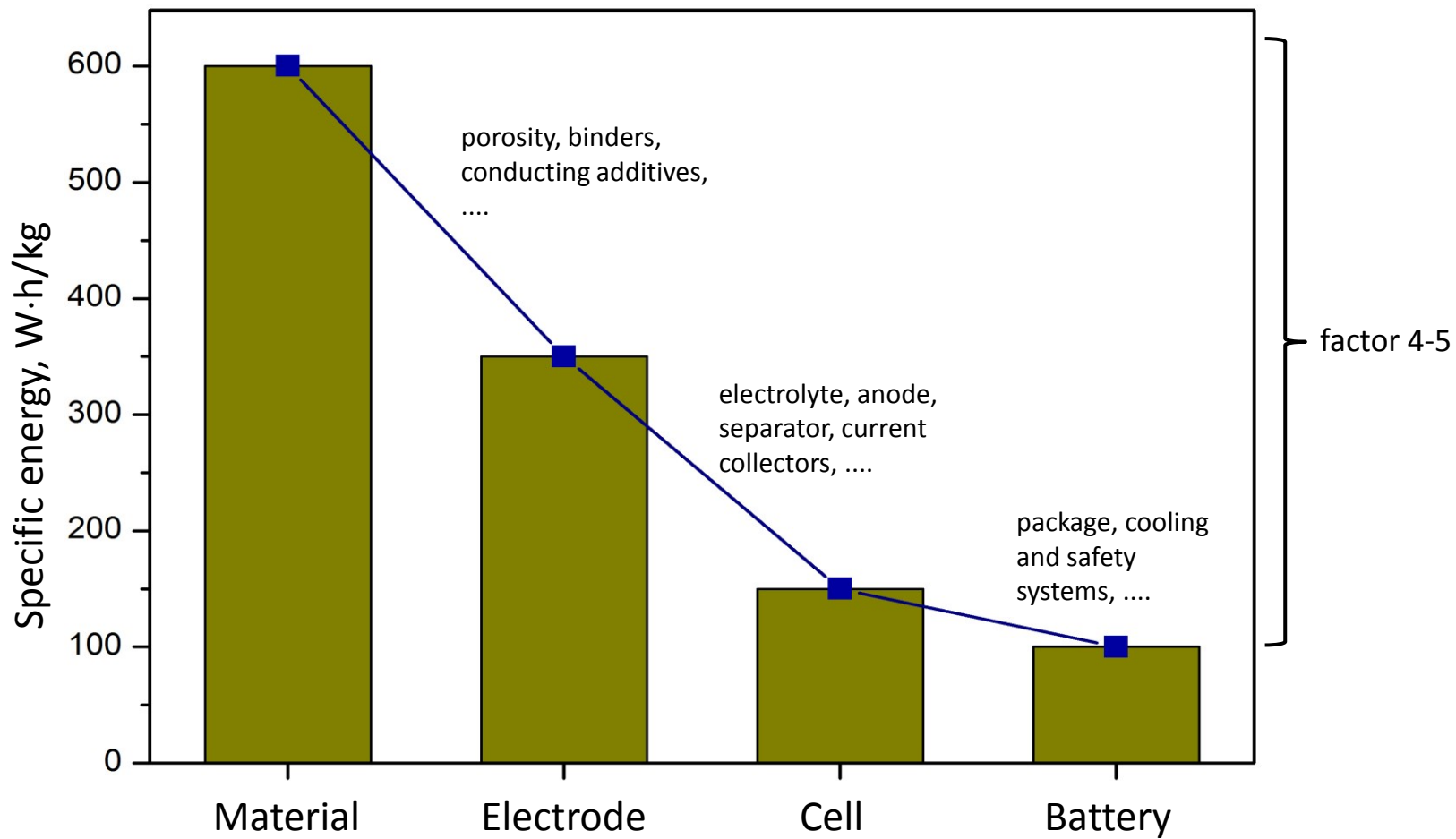
Cathode materials

| Cathode | LCO | LNO | NCA | NMC | LMO | LFP |
|--|------------------|------------------|---|---|---------------------------|-------------------|
| Formula | LiCoO_2 | LiNiO_2 | $\text{LiNi}_{0.85}\text{Co}_{0.1}\text{Al}_{0.05}\text{O}_2$ | $\text{LiNi}_{1/3}\text{Mn}_{1/3}\text{Co}_{1/3}\text{O}_2$ | LiMn_2O_4 | LiFePO_4 |
| Average potential vs Li^+/Li , V | 3.7 | 3.6 | 3.65 | 3.9 | 4.0 | 3.5 |
| Capacity, mA h/g | ~150 | ~180 | ~130 | ~170 | ~110 | ~150 |
| Specific energy, W·h/kg | ~550 | ~650 | ~480 | ~660 | ~440 | ~500 |
| Power | + | 0 | + | 0 | + | + |
| Safety | - | 0 | 0 | 0 | + | ++ |
| Life time | - | 0 | + | 0 | 0 | + |
| Cost | -- | + | 0 | 0 | + | + |

Cathode and anode materials

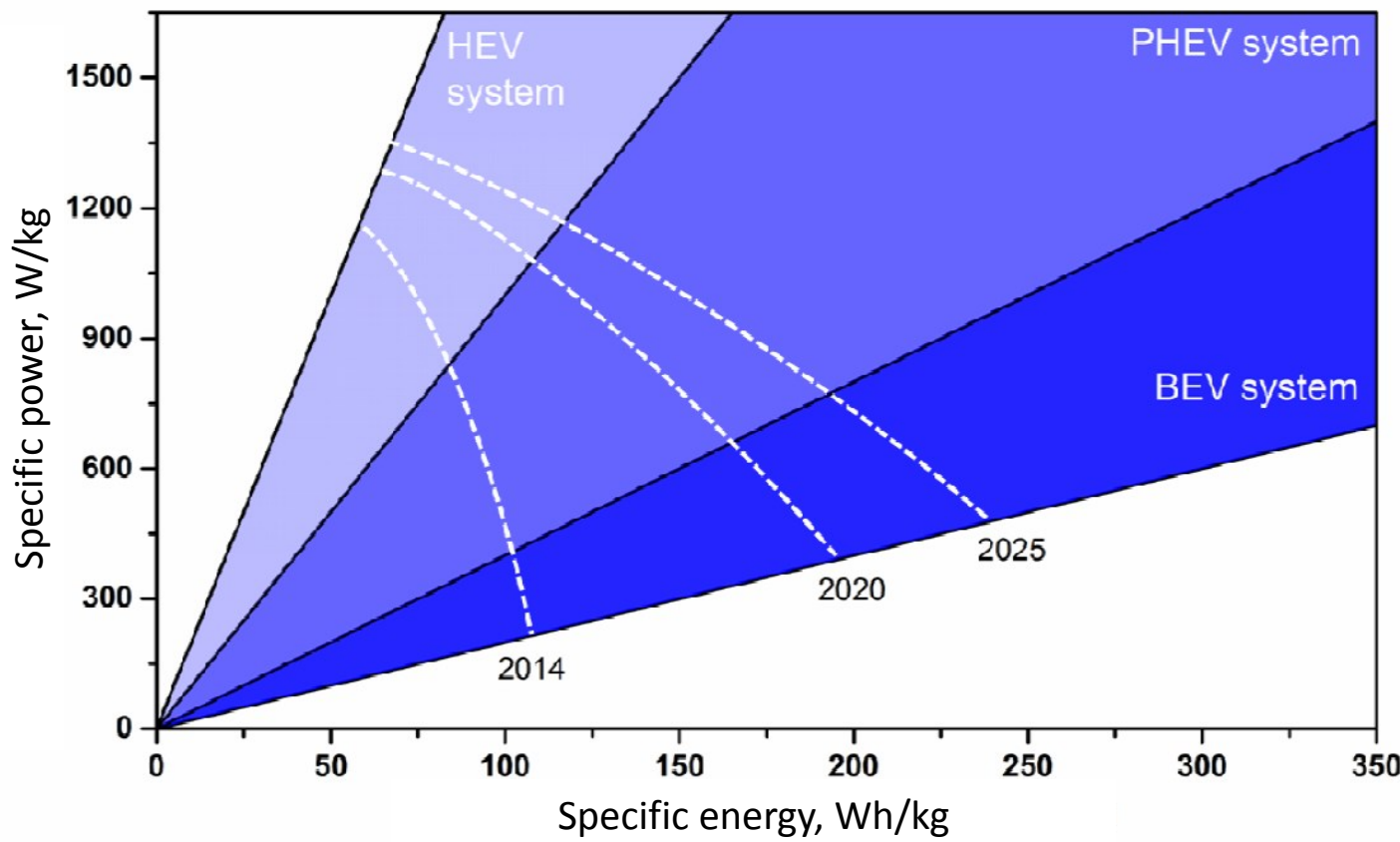


From cathode material to battery



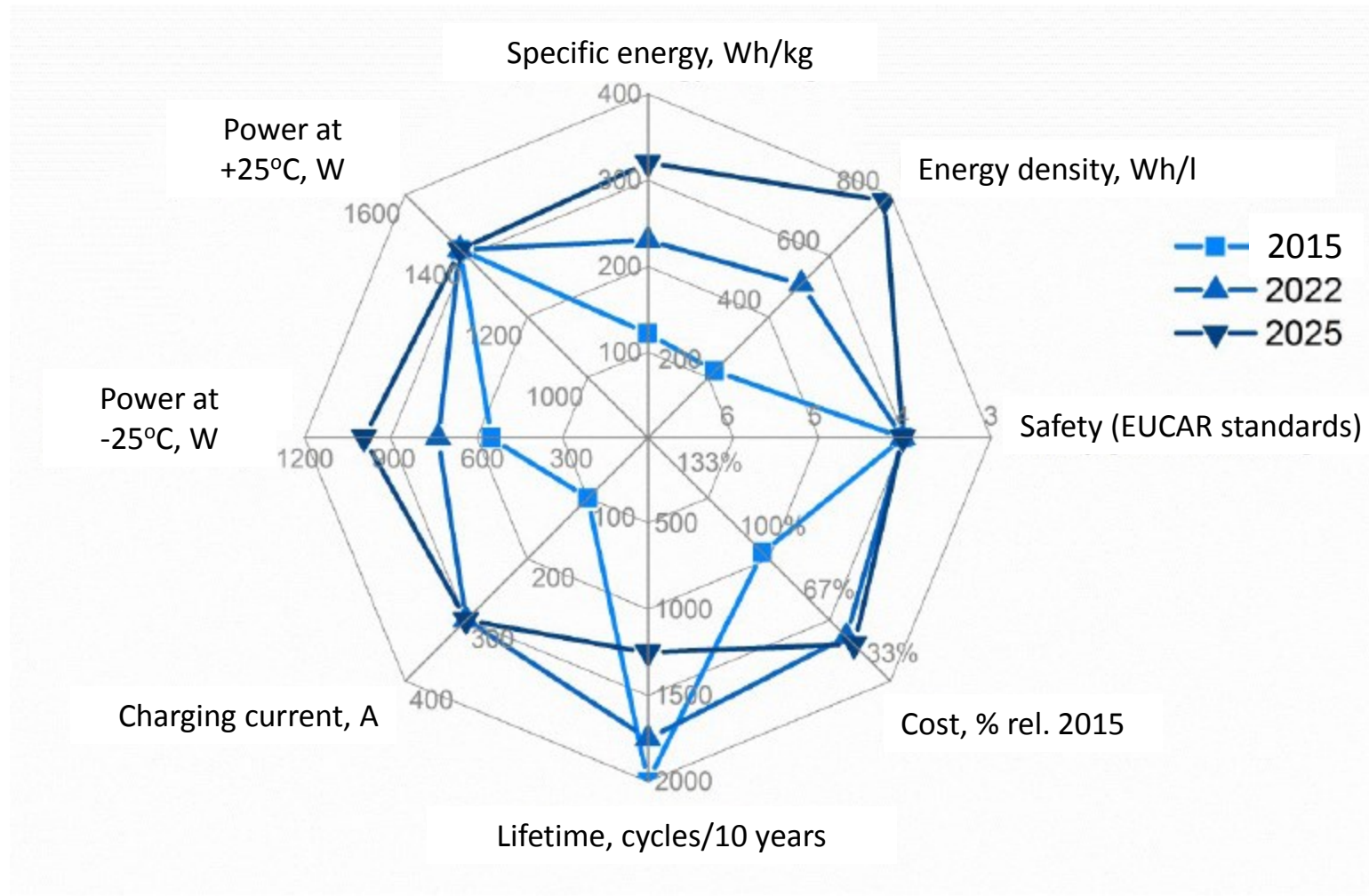
Battery with specific energy of **200 W·h/kg** → cathode with specific energy of **800 – 1000 W·h/kg**

Batteries for automotive applications



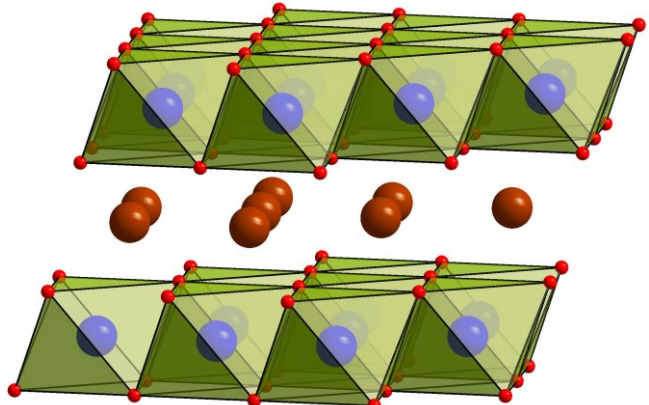
Energy-power diagram for different types of electric vehicles and prospects for 2020 – 2025

Эволюция основных параметров

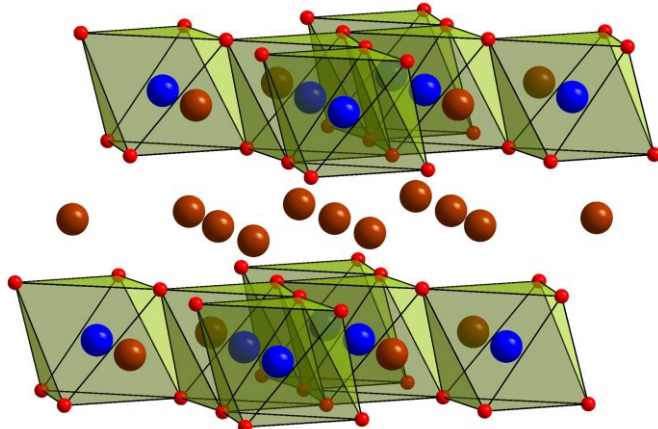
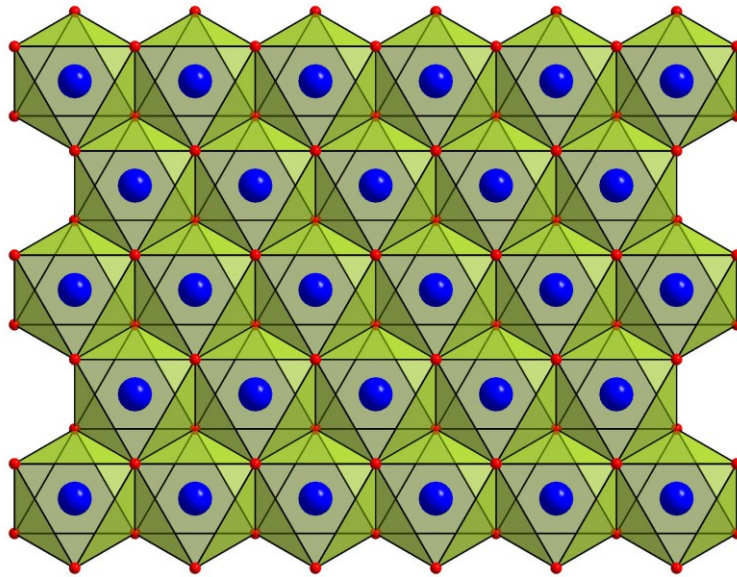


Key performance parameters road map on cell level for fully electrified vehicles from today to 2025.

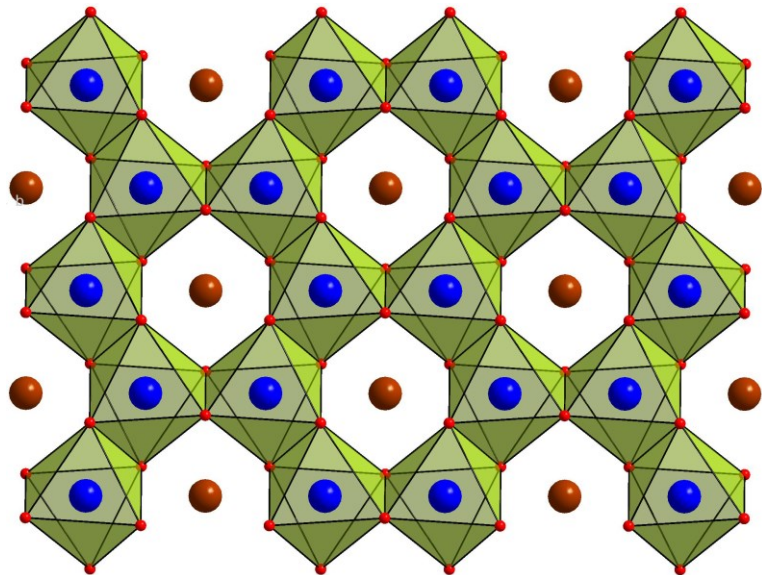
High capacity layered cathodes



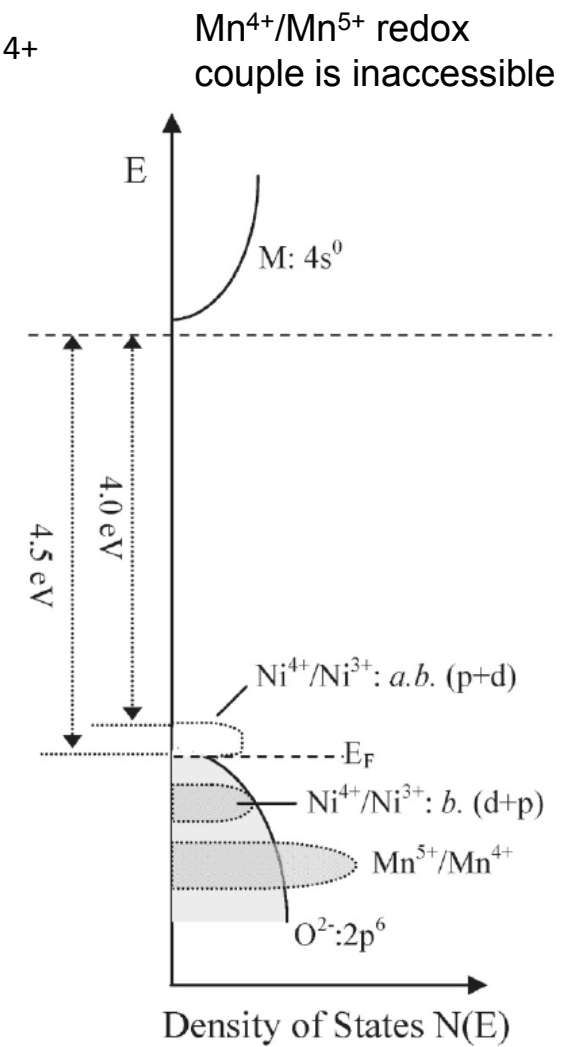
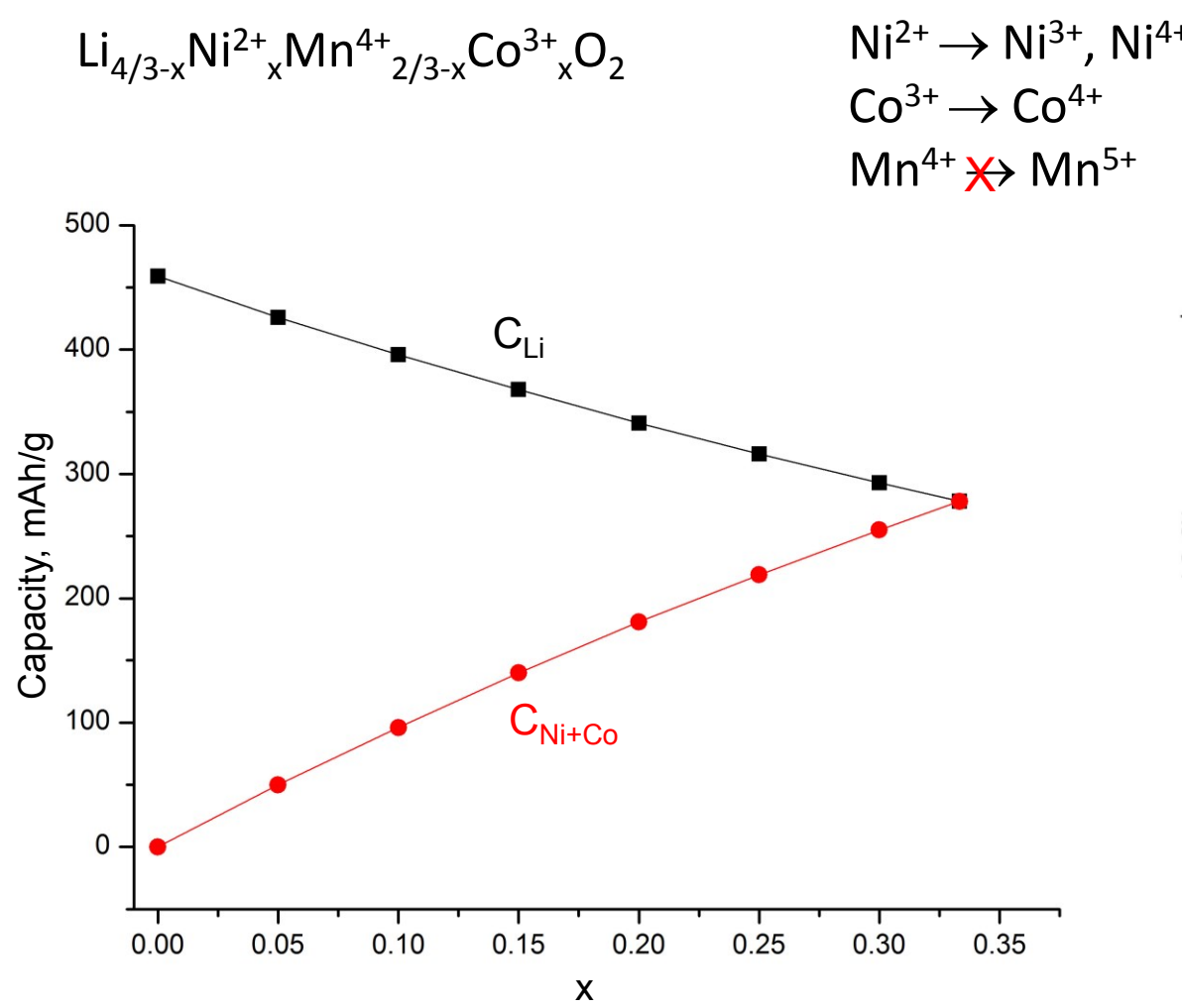
LiCoO_2
 $\text{LiNi}_{1/3}\text{Mn}_{1/3}\text{Co}_{1/3}\text{O}_2$



$\text{Li}_{1+y}(\text{Ni},\text{Mn},\text{Co})_{1-y}\text{O}_2$



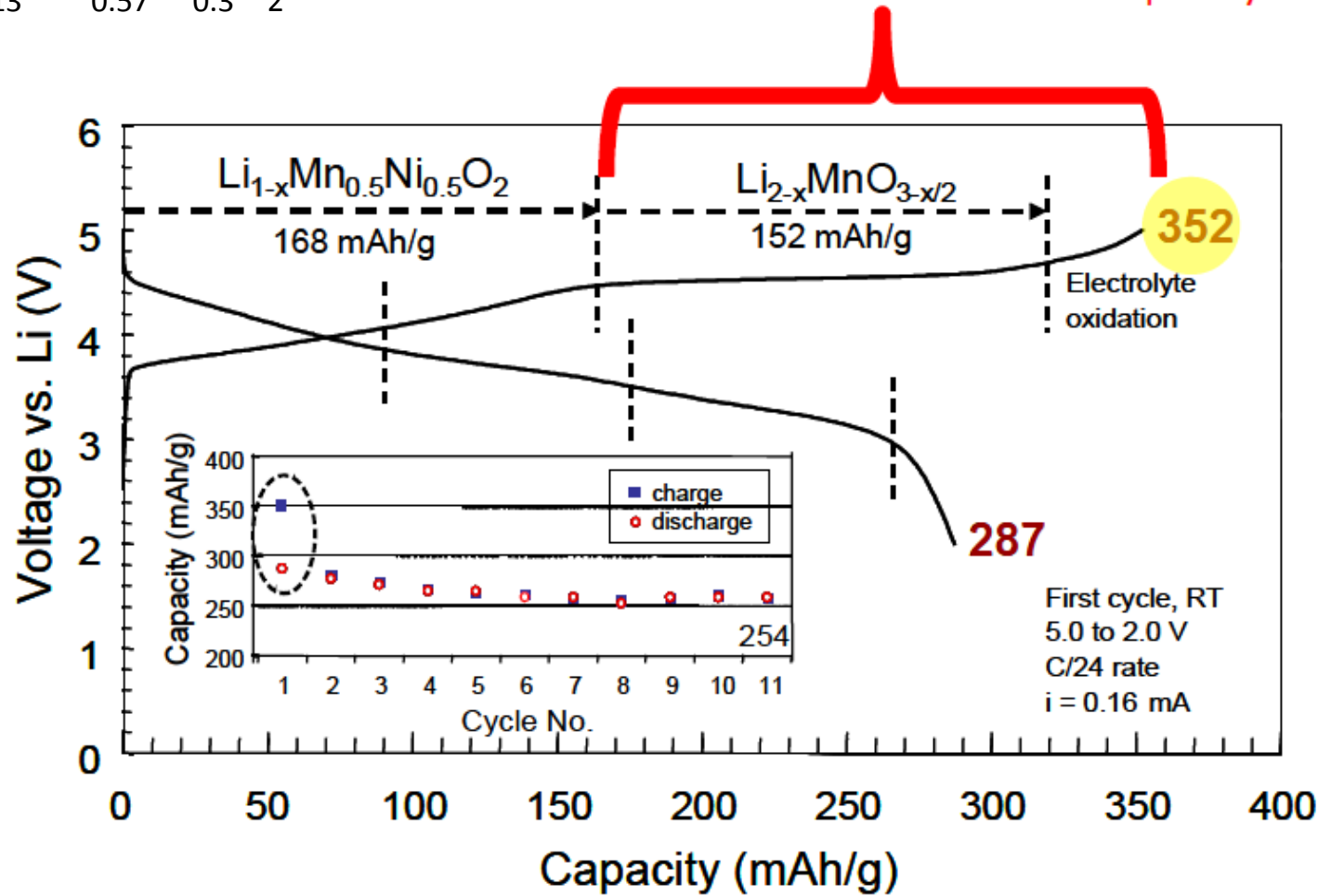
High capacity layered cathodes



High capacity layered cathodes: excess capacity

$\text{Li}_{1.13}\text{Mn}_{0.57}\text{Ni}_{0.3}\text{O}_2$

What is the cause of the excess capacity?



Lattice oxygen oxidation

Identification of cathode materials for lithium batteries guided by first-principles calculations

G. Ceder, Y.-M. Chiang, D. R. Sadoway, M. K. Aydinol,
Y.-I. Jang & B. Huang

The replacement with non-transition metals is driven by the realization that oxygen, rather than transition-metal ions, function as the electron acceptor upon insertion of Li.

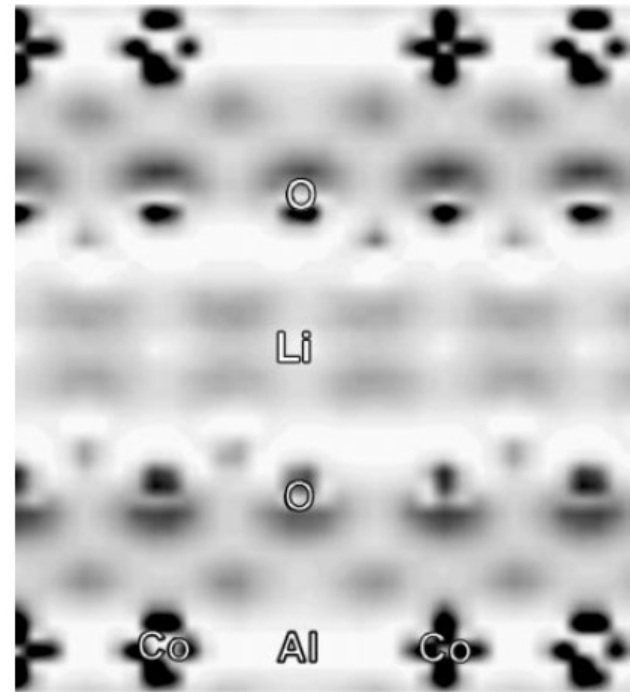
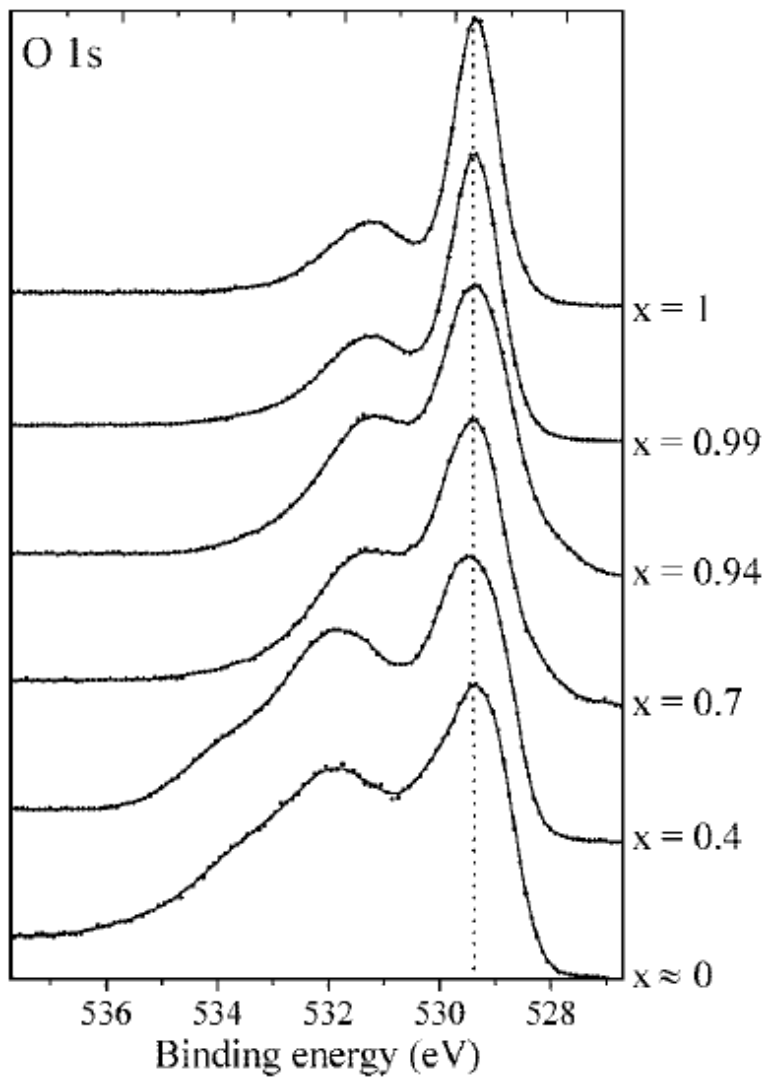


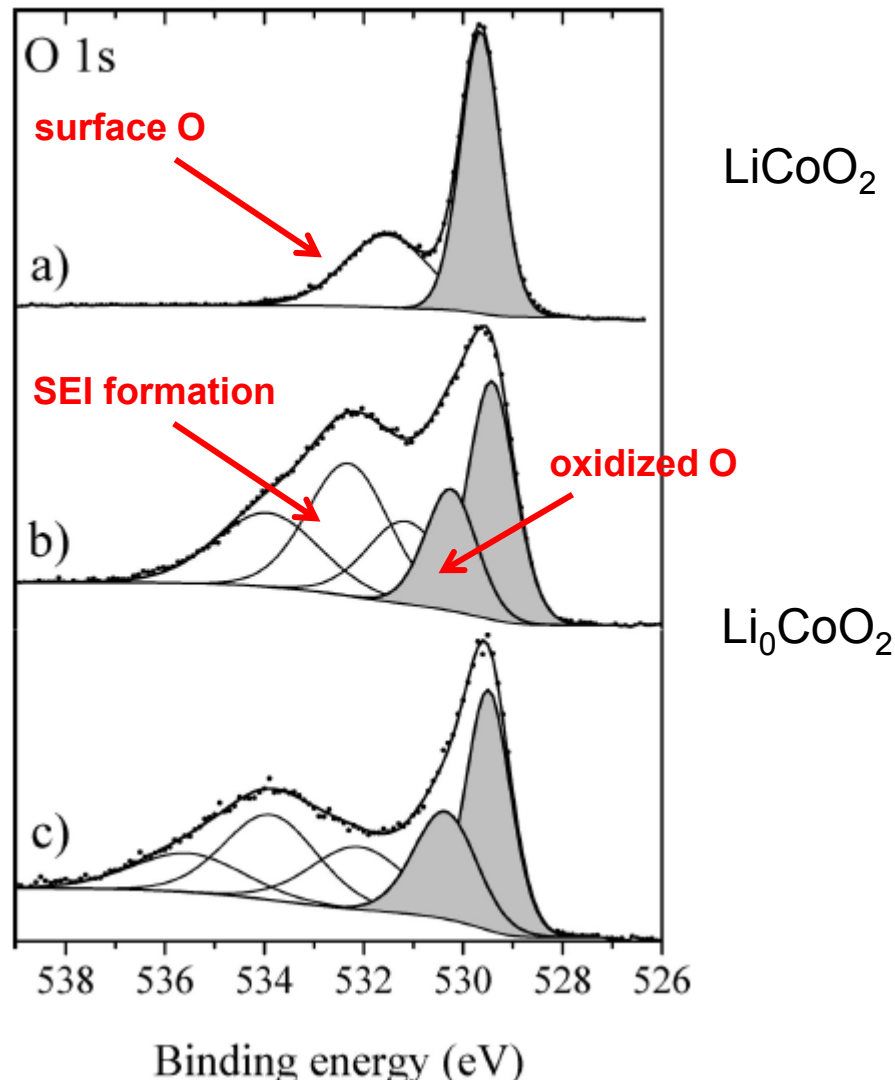
Figure 1 Positive part of the electron density difference between $\text{Li}(\text{Al}_{0.33}\text{Co}_{0.67})\text{O}_2$ and $(\text{Al}_{0.33}\text{Co}_{0.67})\text{O}_2$ in a plane perpendicular to the direction of layering in the structure. Darker indicates larger electron density.

NATURE | VOL 392 | 16 APRIL 1998

Lattice oxygen oxidation

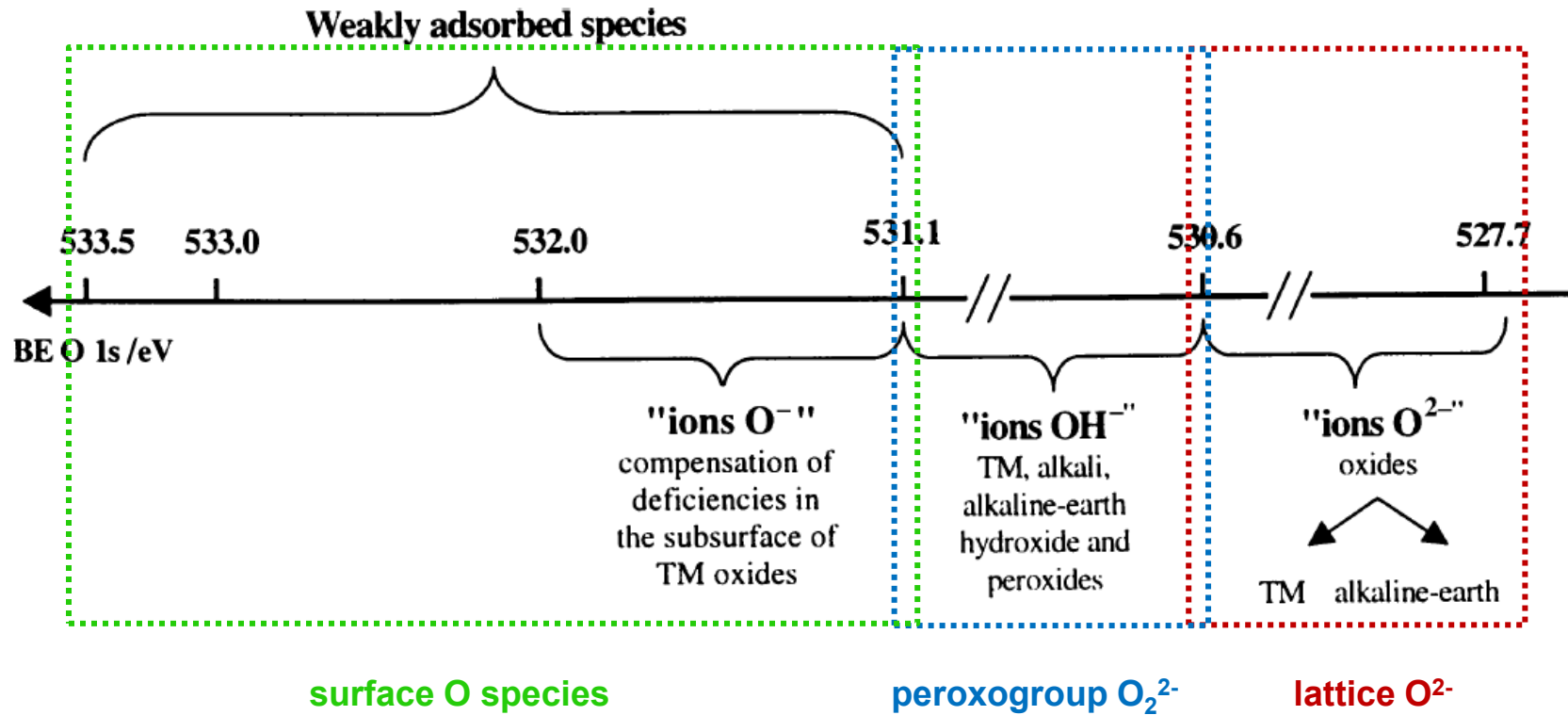


Li_xCoO_2 XPS O1s

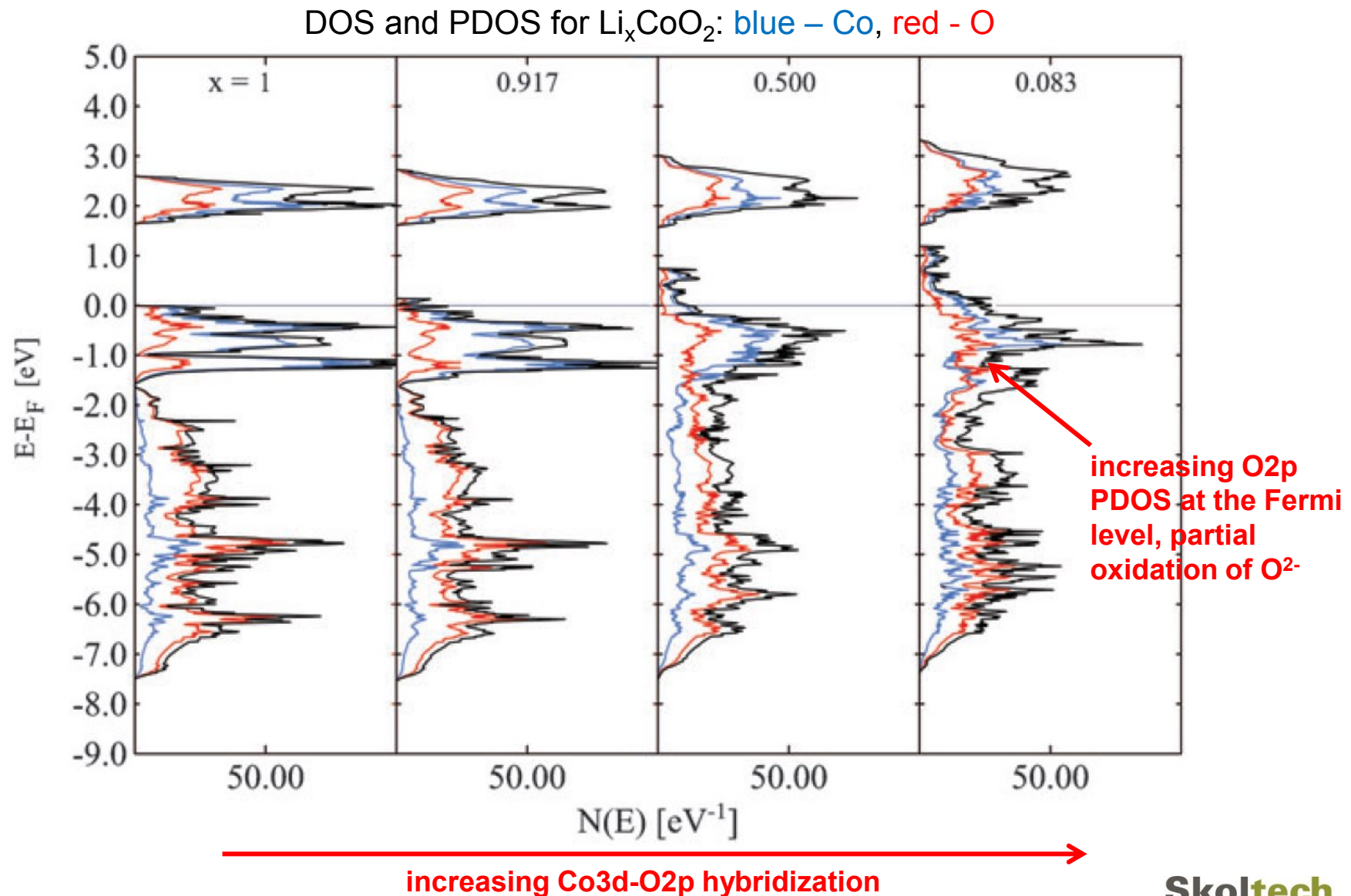


L.Daheron et al., Chem.Mater., 20, 583, 2008

Lattice oxygen oxidation

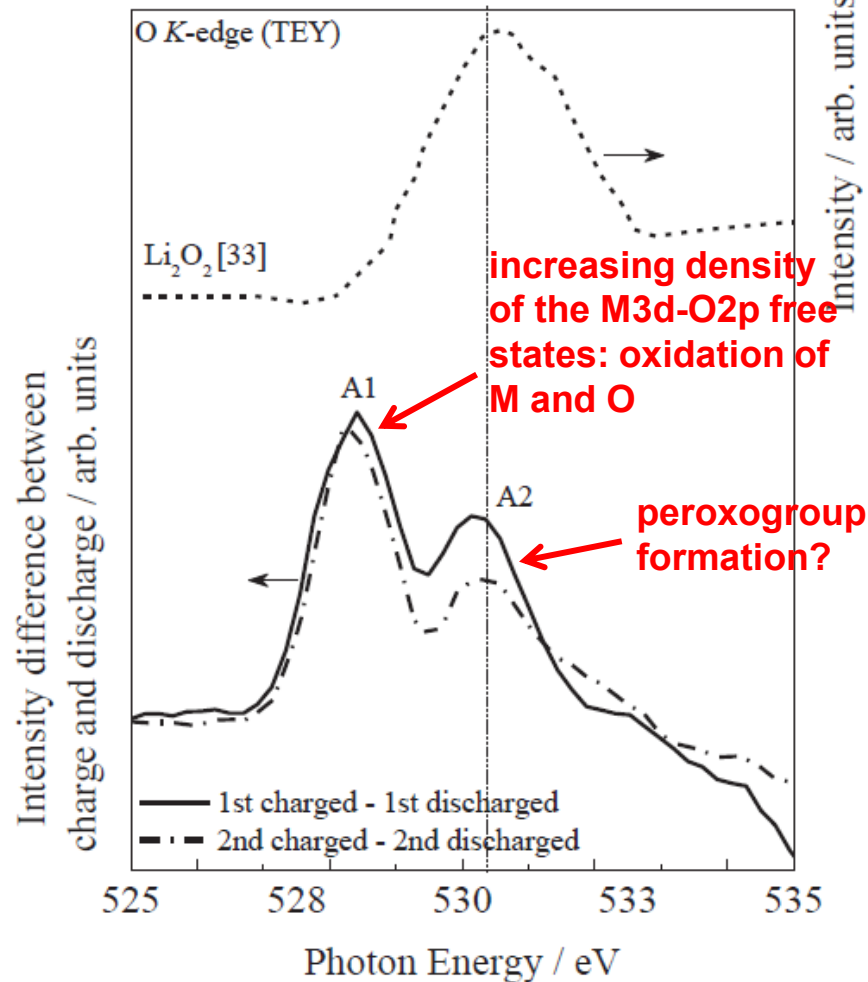
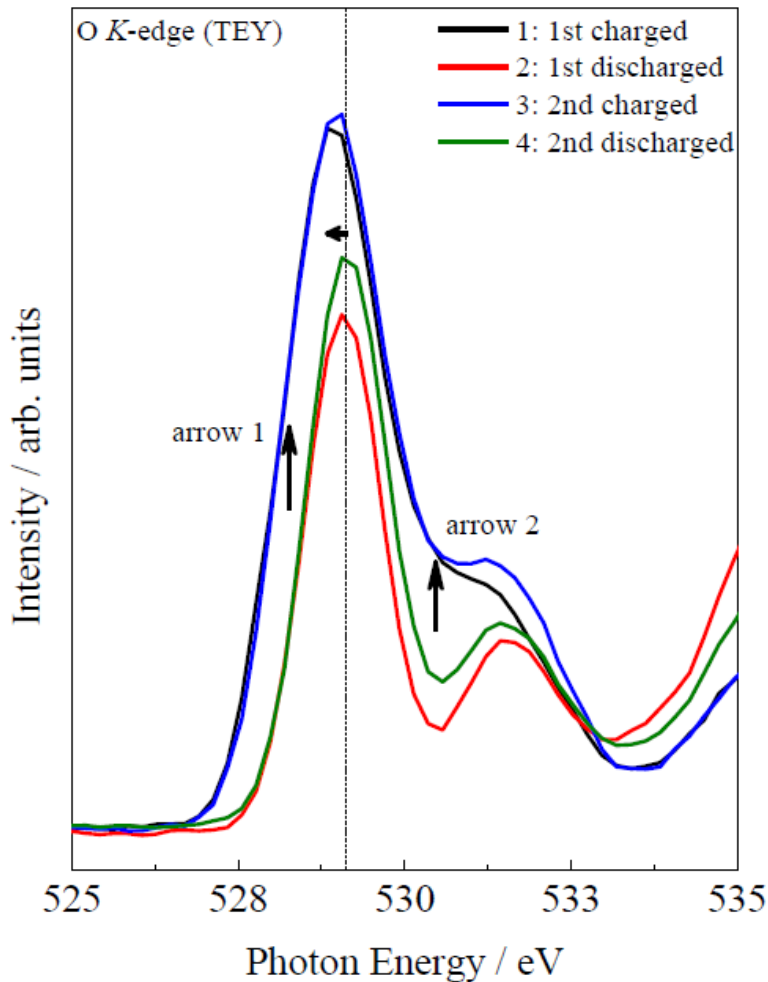


Lattice oxygen oxidation

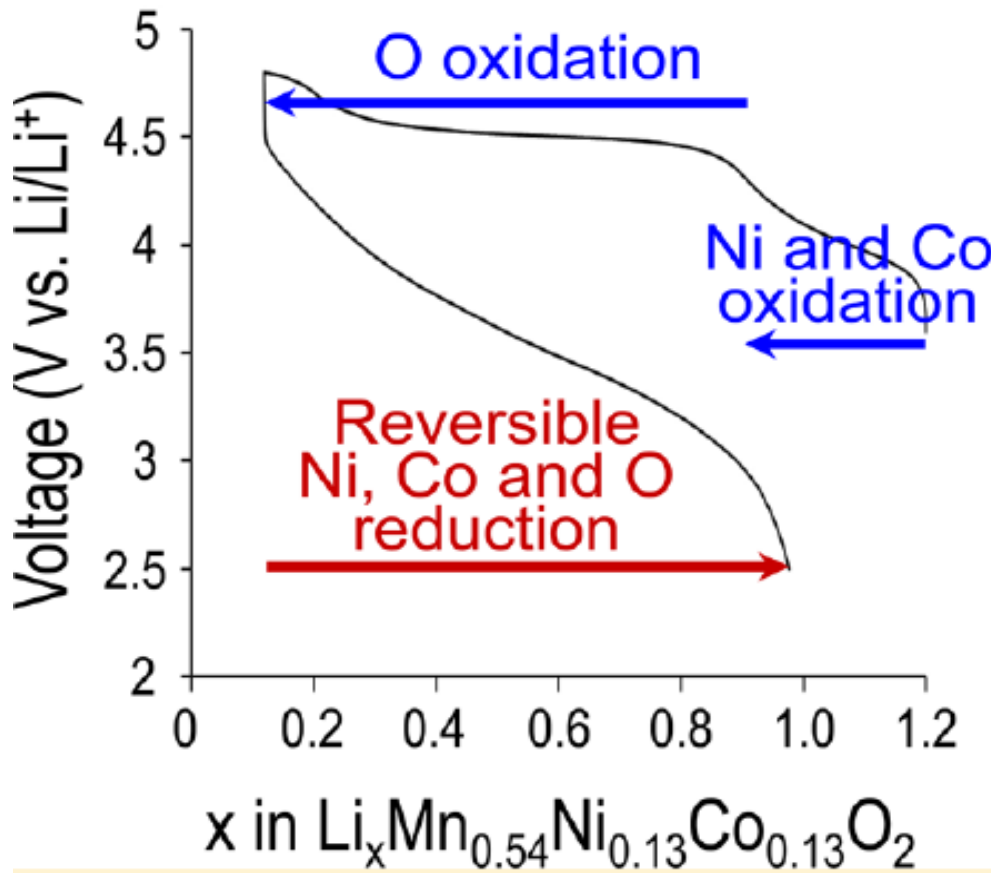


Lattice oxygen oxidation

Li-rich NMC: O-K edge XAFS



Lattice oxygen oxidation



Two redox processes:

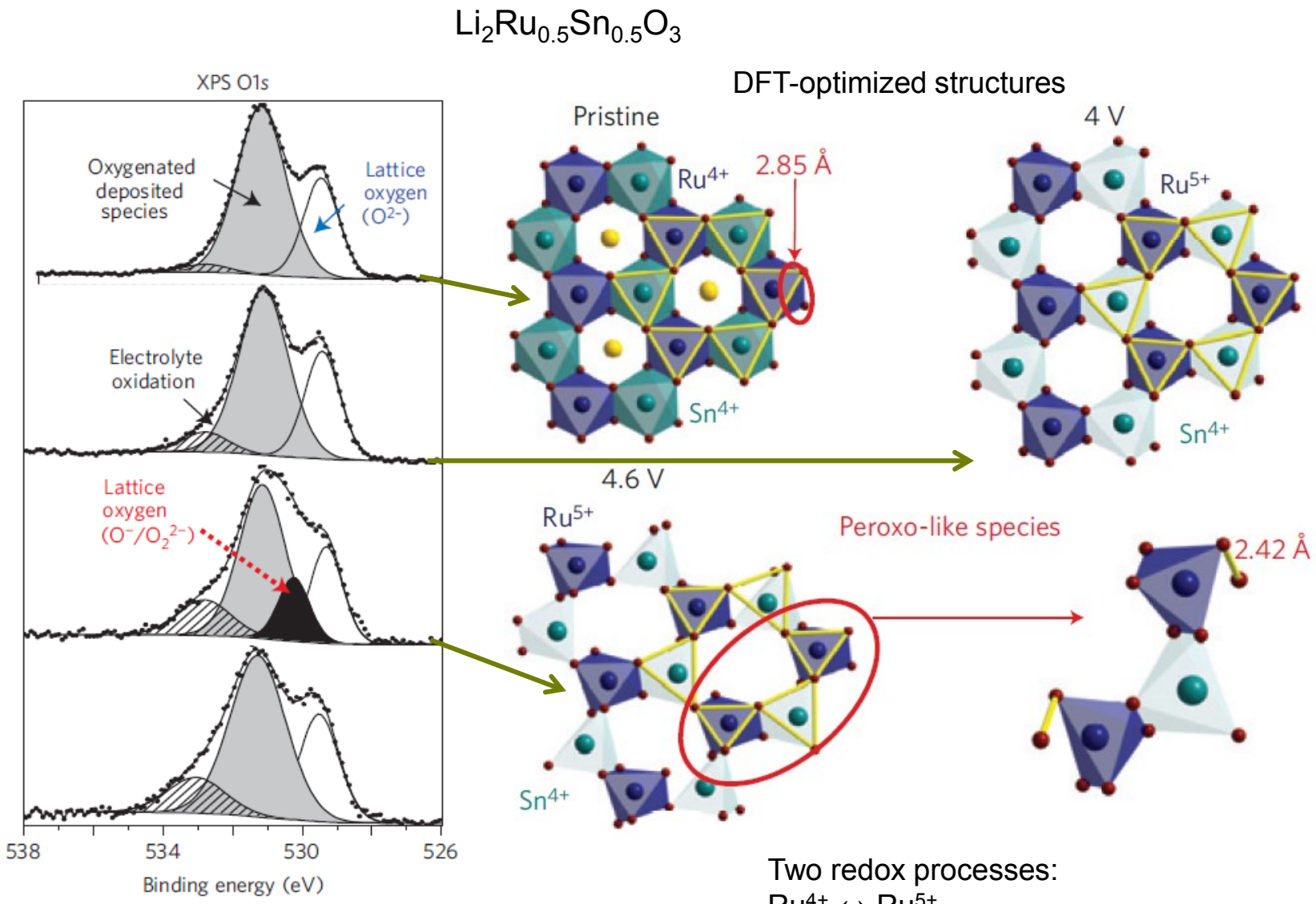


(Mn^{4+} is neither oxidized nor reduced)

Reversible oxygen oxidation

XANES and EXAFS on Ni, Co and Mn-K edges

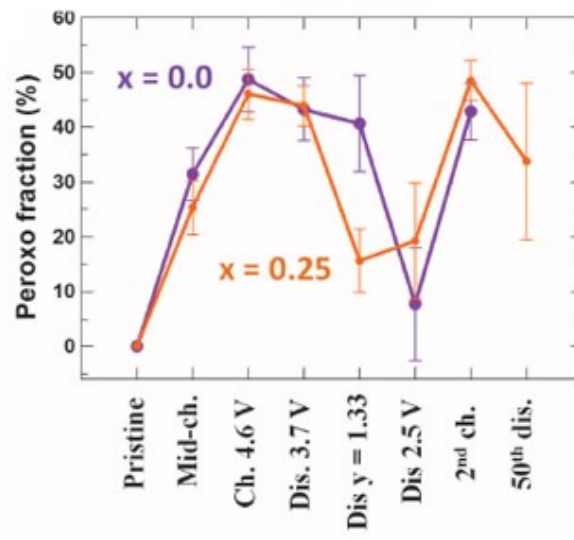
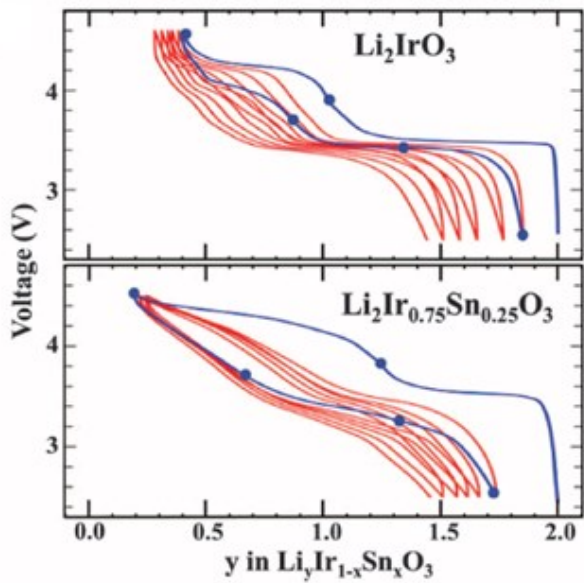
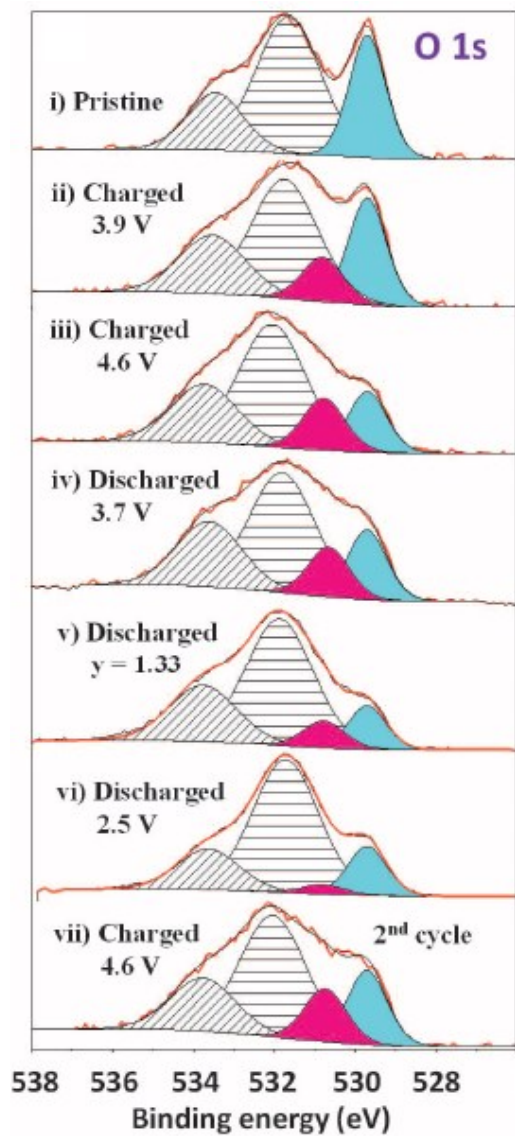
Formation of O_2^{n-}



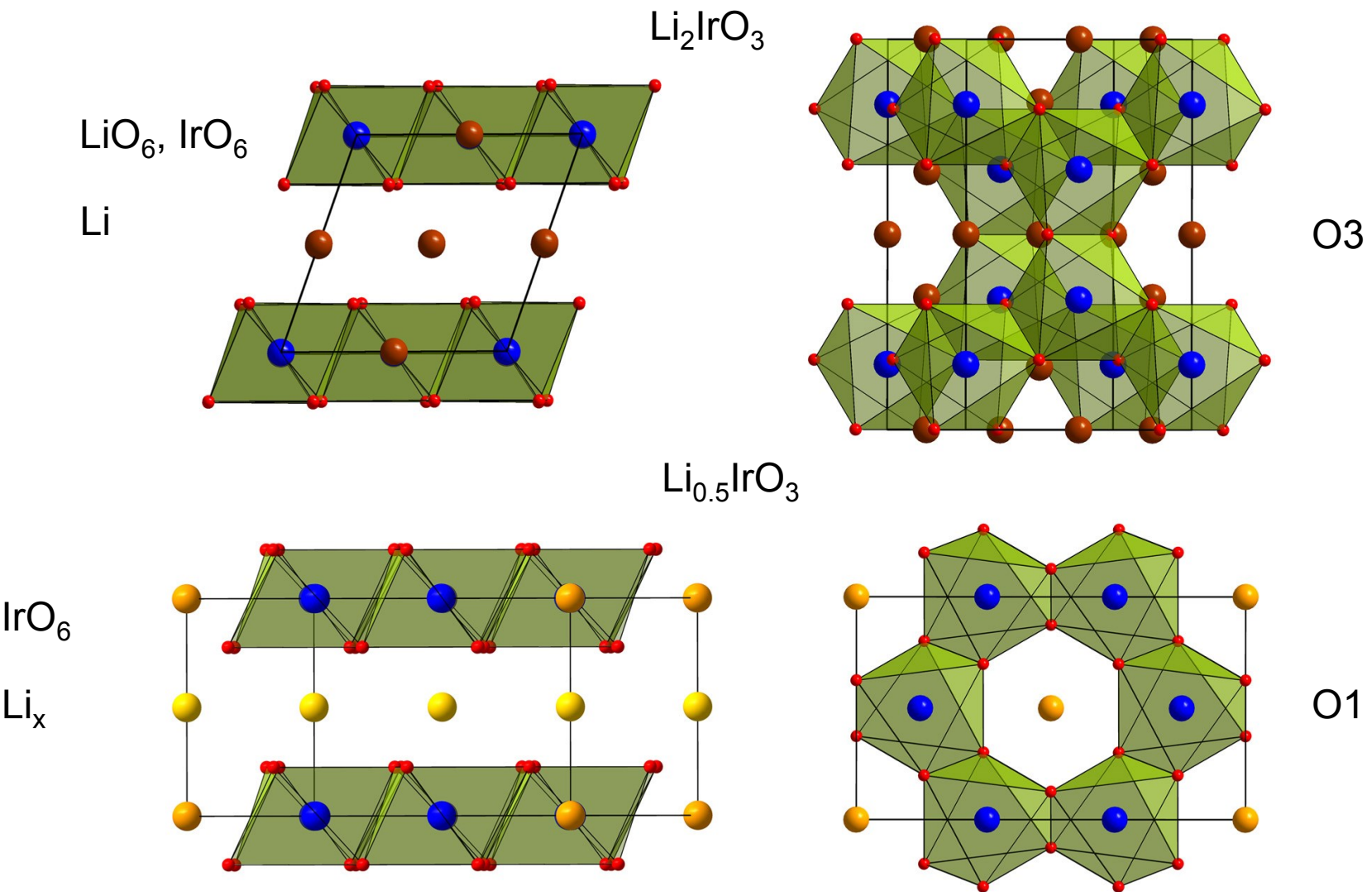
Formation of O₂ⁿ⁻



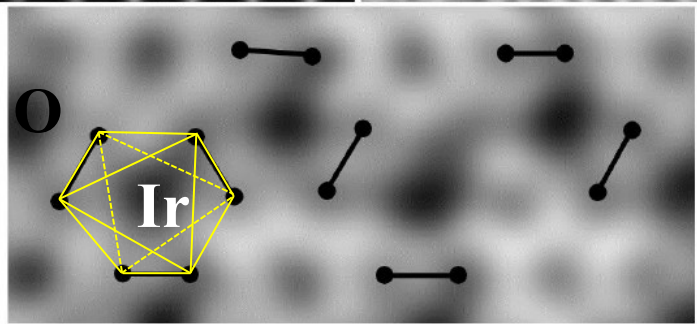
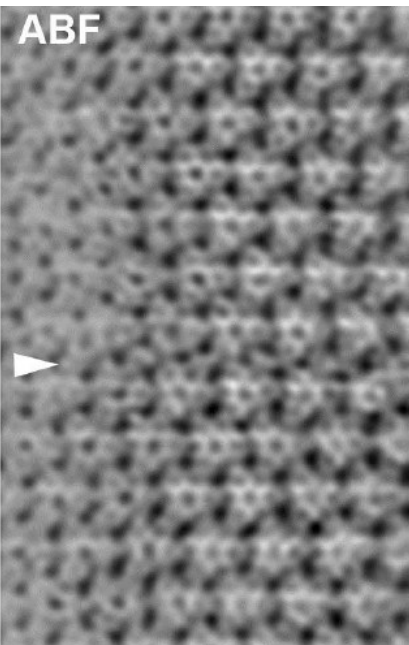
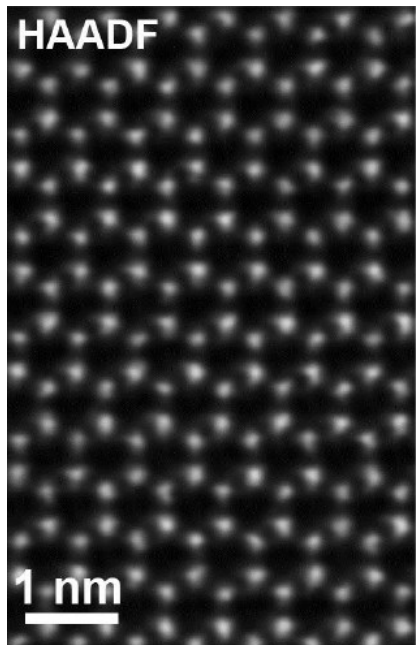
Two redox processes:



Formation of O₂ⁿ⁻

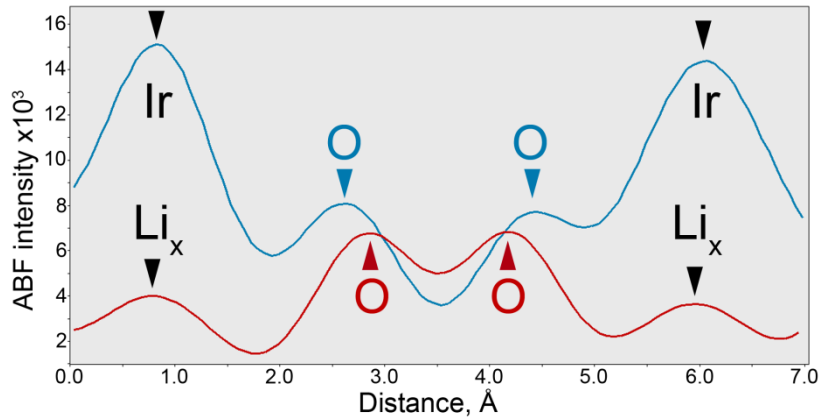


Formation of O₂ⁿ⁻



HAADF- and ABF-STEM for Li_{0.5}IrO₃ charged to 4.5V

$\text{Li}_2\text{IrO}_3 \rightarrow \text{Li}_{0.5}\text{IrO}_3$: oxidation of $\text{Ir}^{4+} \rightarrow \text{Ir}^{5+}$ and $\text{O}^{2-} \rightarrow \text{O}_2^{\text{n}-}$ ($n < 4$), shortening the O-O distances



Projected O-O distances from ABF-STEM:
short: 1.56(1) Å long: 1.83(1) Å

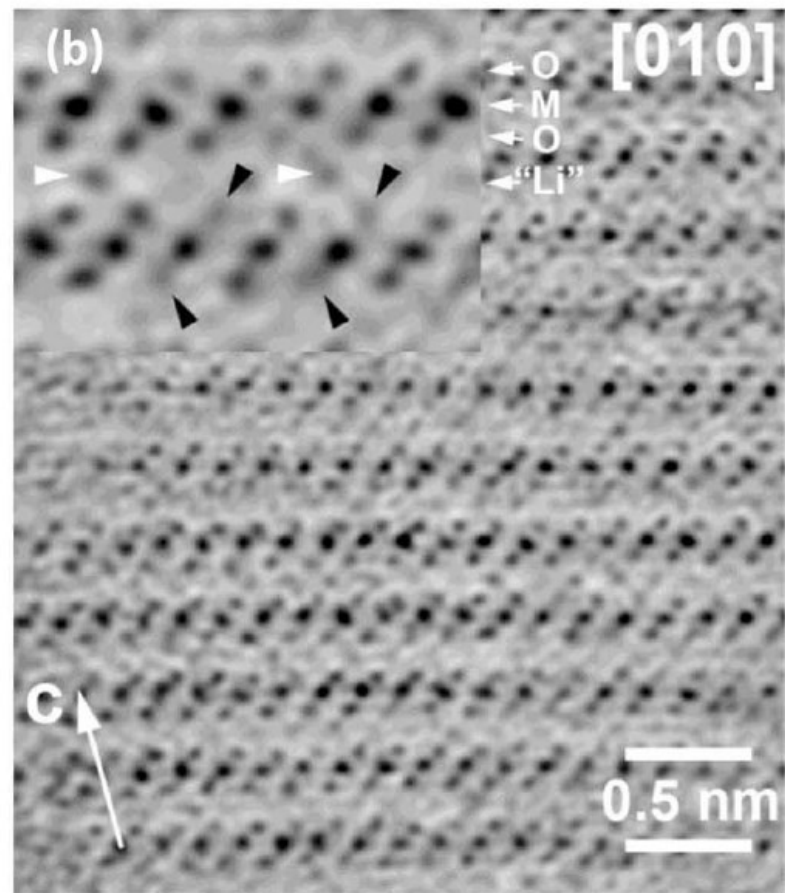
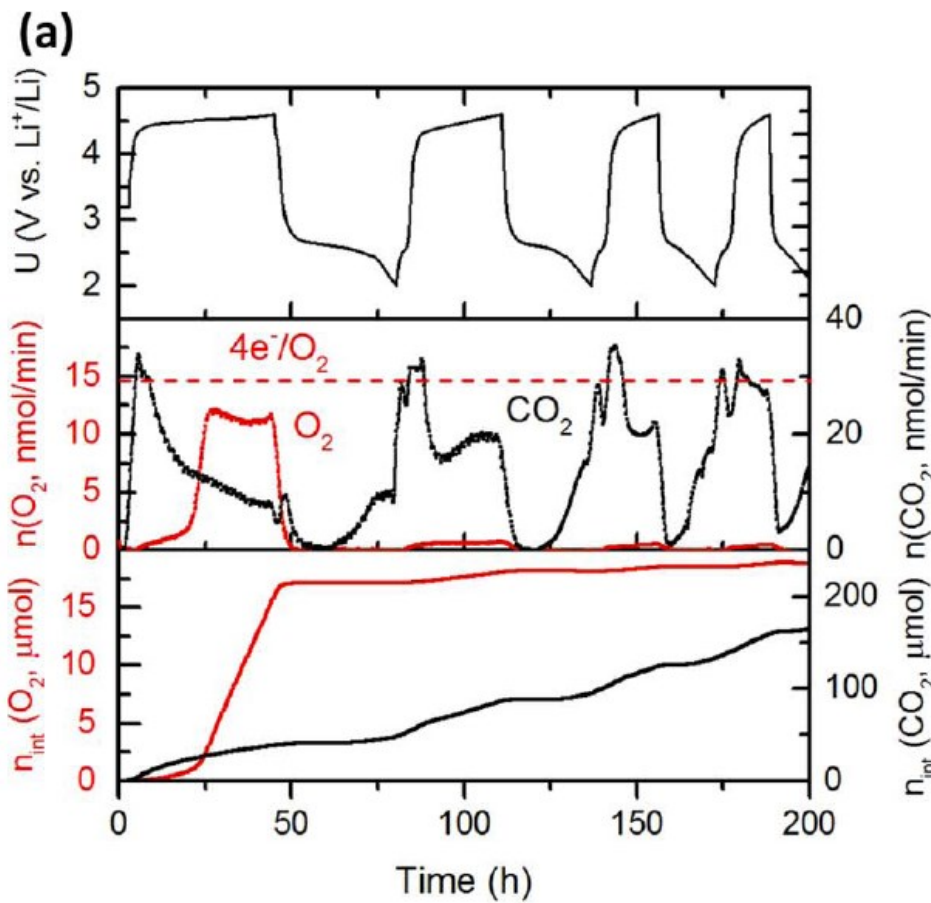
Projected O-O distances from DFT ($\text{Li}_{0.5}\text{IrO}_3$):
short: 1.48 Å long: 1.85 Å

Formation of O₂ⁿ⁻

Table 1. Average O-O distances obtained by DFT, NPD, and TEM. "Short" refers to two oxygen atoms between two nearest-neighbor Ir atoms, as viewed in the [001] projection in Fig. 3, E and F. "Long" refers to distances at which the oxygen atoms lie between an Ir atom and a vacancy. In all cases, the distances are averages for the structure. Projected distances are shown for the O1 structure only. N/A, not applicable; ND, not determined.

| Sample | O-O distance (Å) | | O-O distance in [001] projection (Å) | |
|---|------------------|---------|--------------------------------------|---------|
| | Short | Long | Short | Long |
| Li ₂ IrO ₃ | | | | |
| Neutron | 2.77(2) | 2.84(2) | N/A | N/A |
| DFT | 2.74 | 2.89 | N/A | N/A |
| Li _{0.5} IrO ₃ | | | | |
| Neutron | 2.45(2) | 2.73(4) | 1.42(1) | 1.86(3) |
| DFT | 2.54 | 2.77 | 1.51 | 1.88 |
| TEM | ND | ND | 1.56 | 1.83 |
| LiNi _{1/3} Mn _{1/3} Co _{1/3} O ₂ * | 2.686 | 2.686 | N/A | N/A |
| Li _{0.04} Ni _{1/3} Mn _{1/3} Co _{1/3} O ₂ * | 2.553 | 2.553 | N/A | N/A |

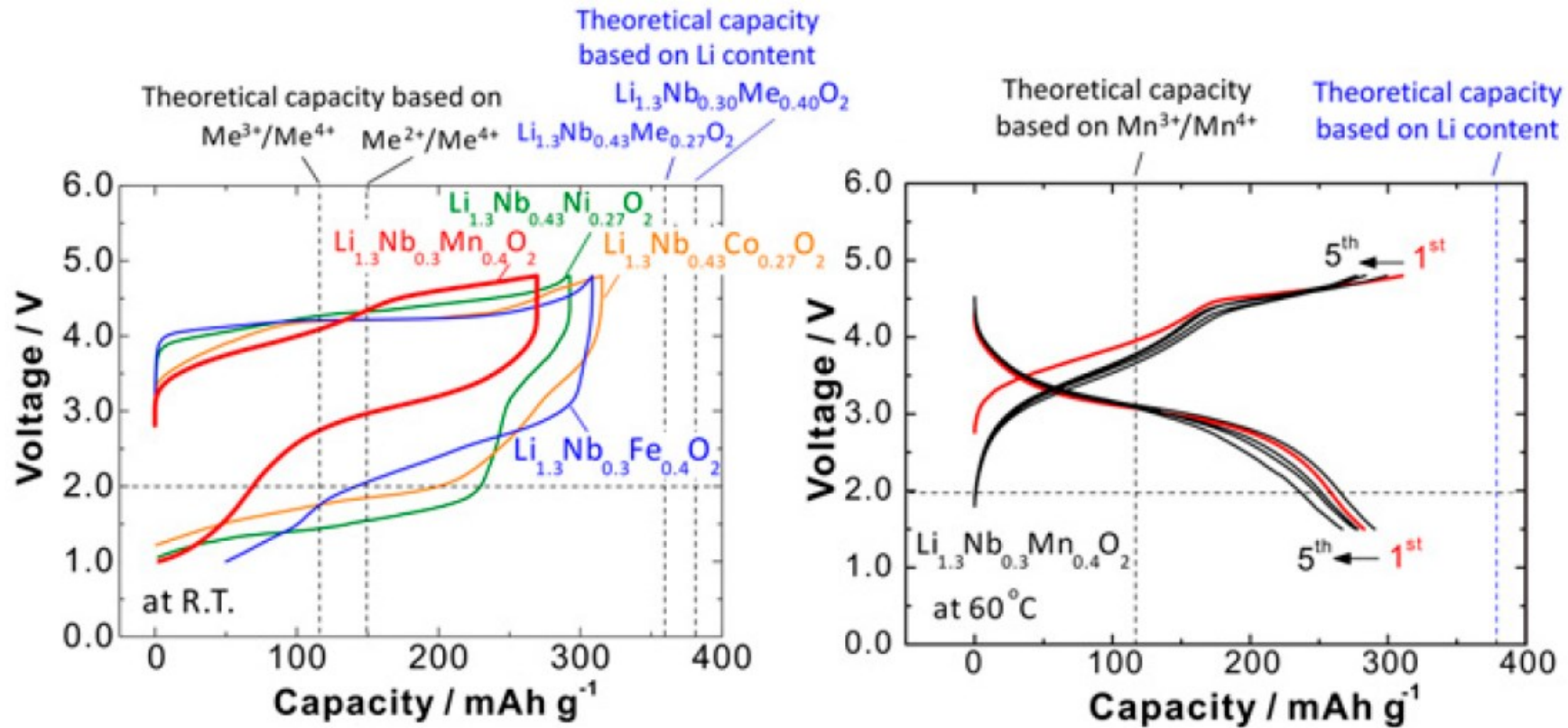
Oxygen evolution and thermal runaway



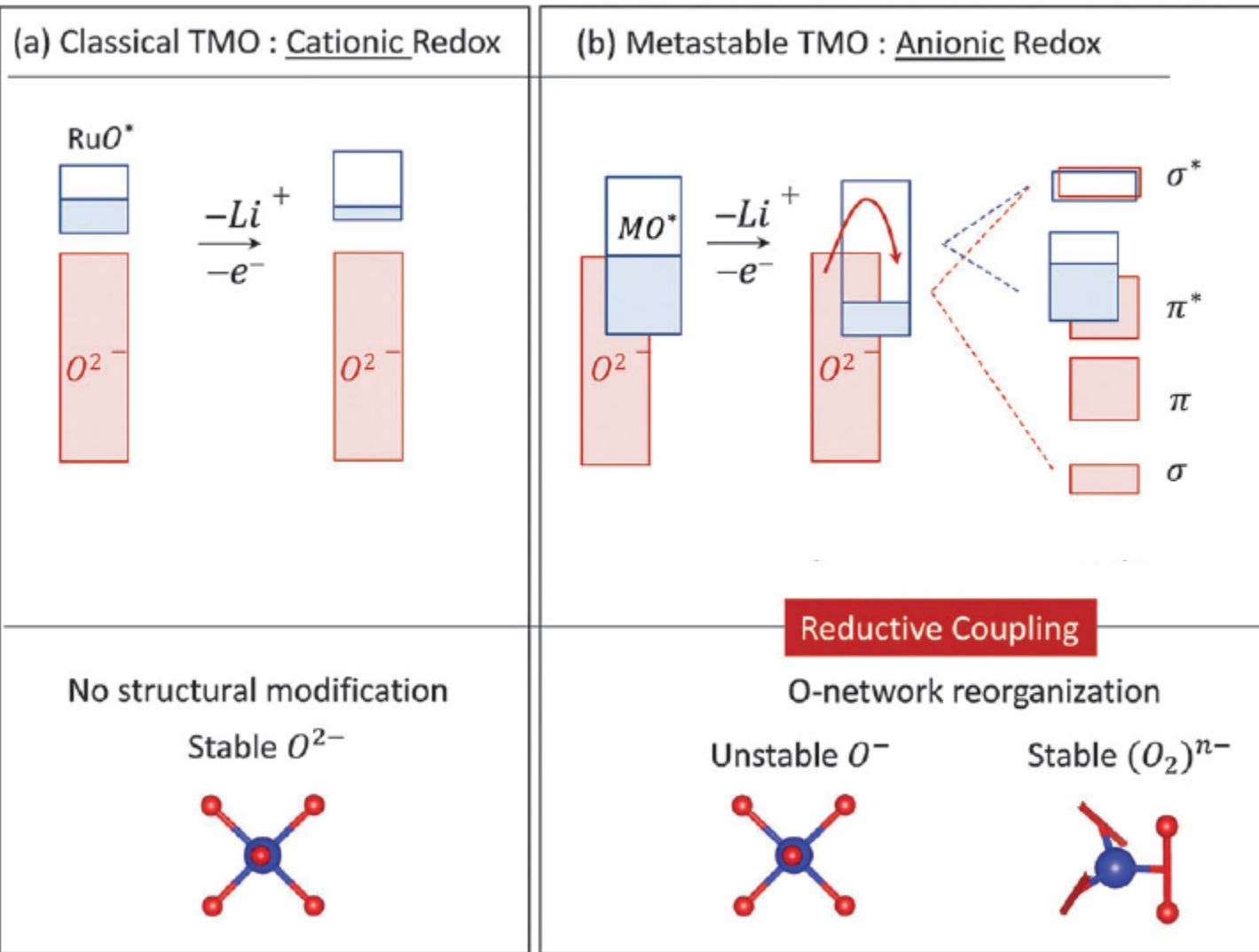
Irreversible capacity solely due to the oxygen evolution

McCalla et al., JES, 162, A1341 (2015)

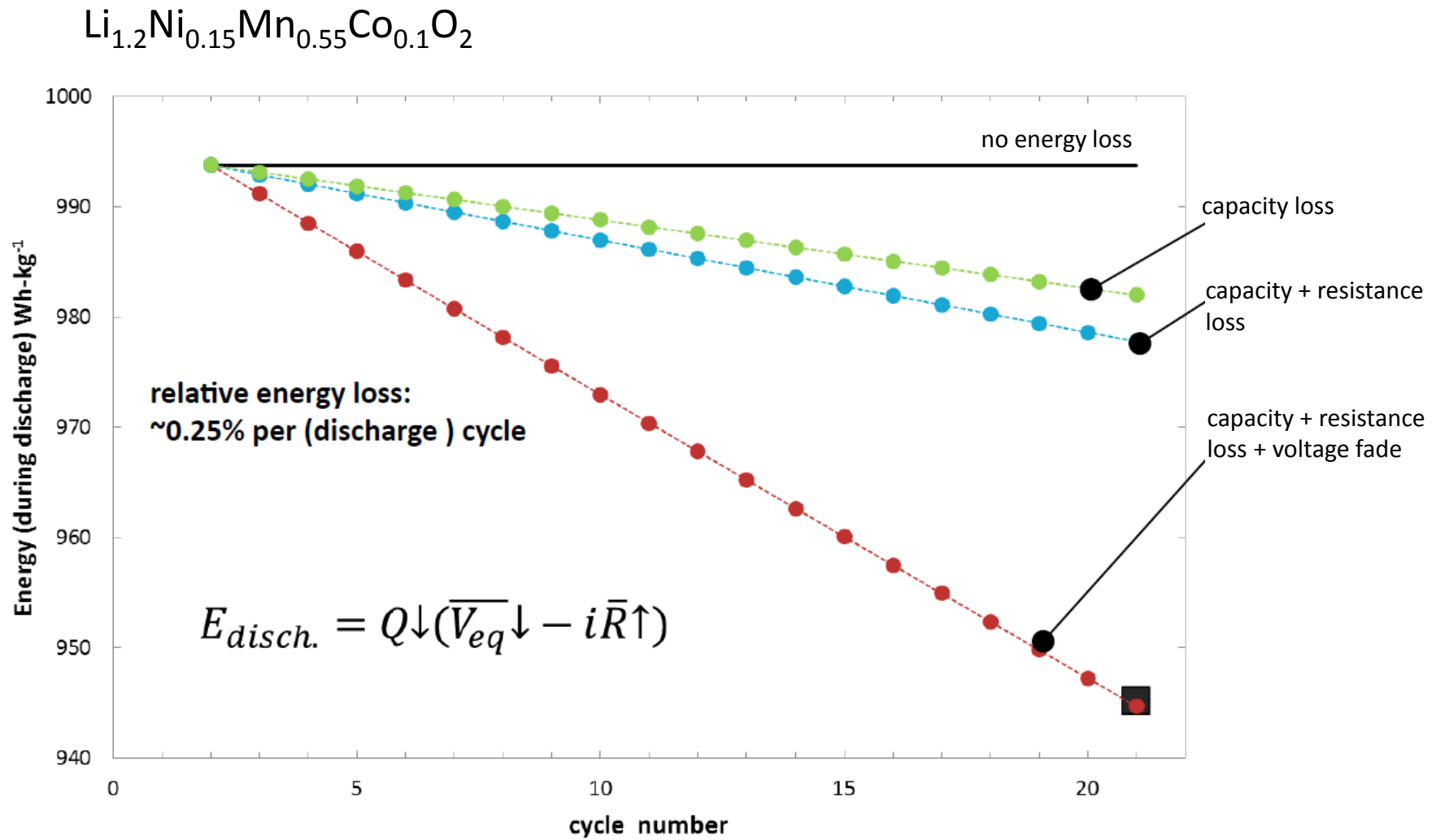
Reversible oxygen oxidation



Metastable anionic redox reaction



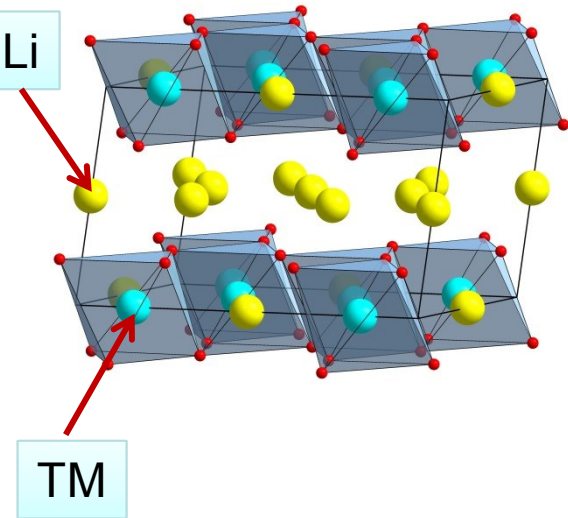
High capacity layered cathodes: energy losses



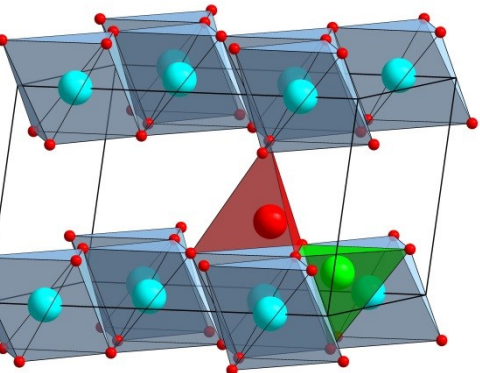
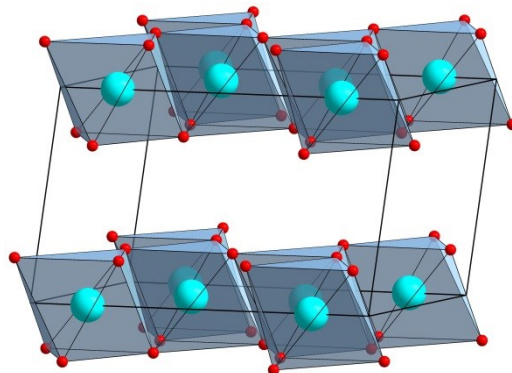
High capacity layered cathodes: energy losses

- Do the TM cations migrate?
- What are the host positions?
- Is the migration reversible?

Pristine Li_2MO_3
M – 3d, 4d transition metal

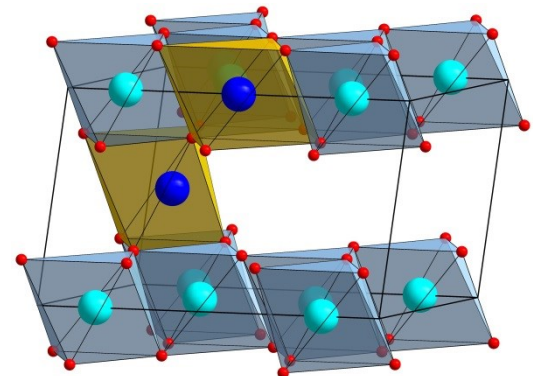


Hypothetic
fully delithiated

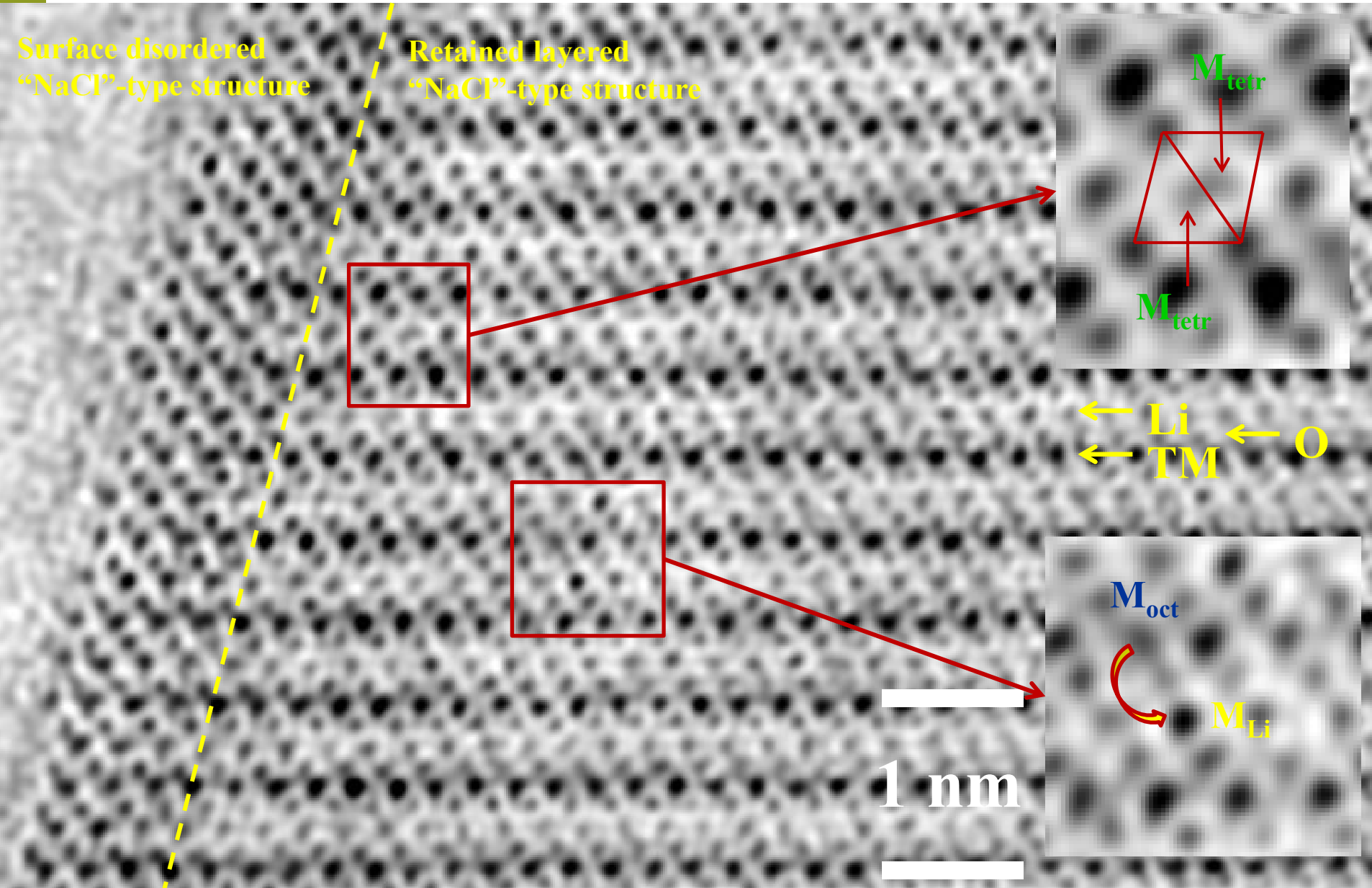


Migration of the M cations
to intra- and interlayer
tetrahedral sites

Migration of the M cations
to intra- and interlayer
octahedral sites

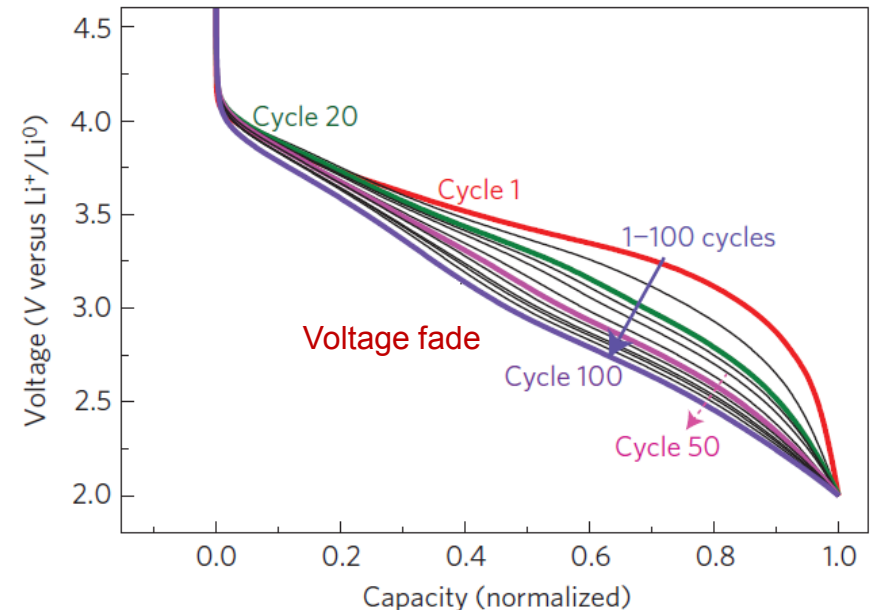
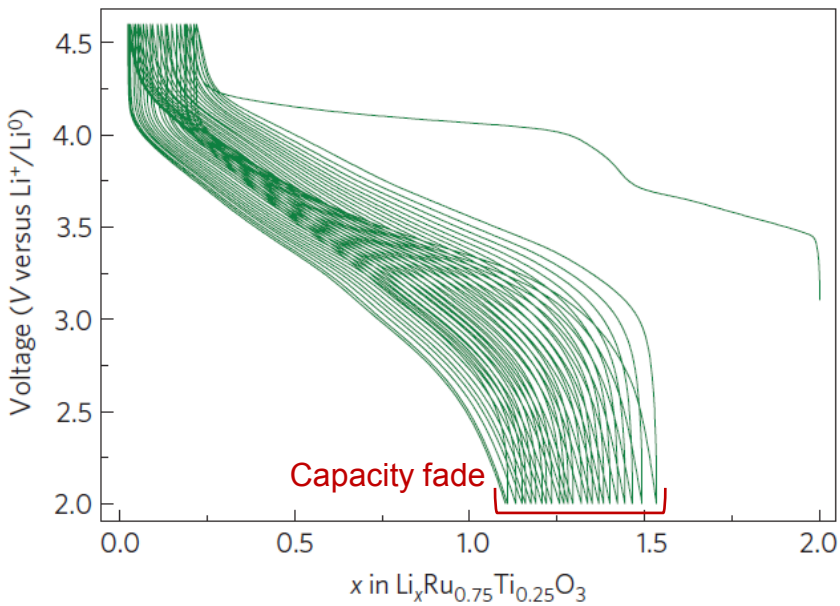


High capacity layered cathodes: energy losses



Capacity and voltage fade – $\text{Li}_2\text{Ru}_{0.75}\text{Ti}_{0.25}\text{O}_3$

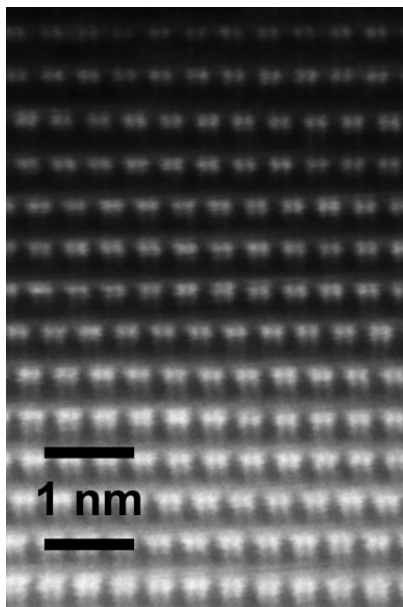
100 charge/discharge cycles – discharge curves



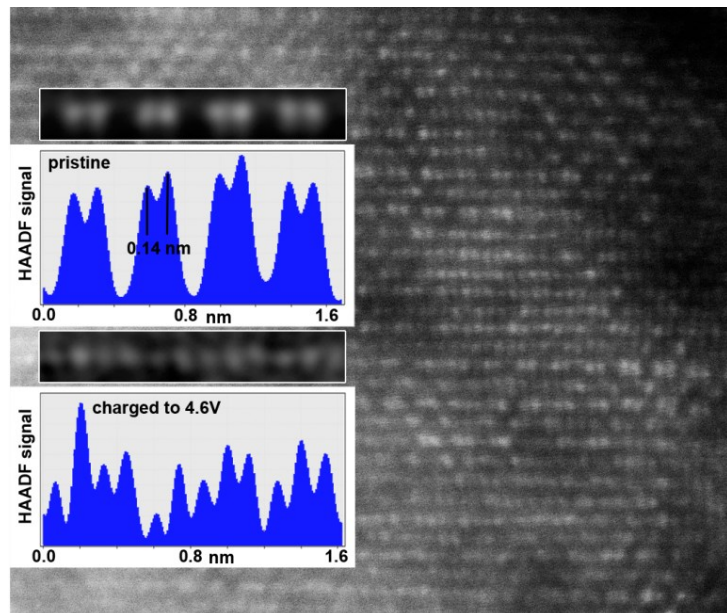
Sathiya, Abakumov, Foix, Rousse, Ramesha, Saubanère, Doublet, Vezin, Laisa, Prakash, Gonbeau, Van Tendeloo, Tarascon, *Nature Mater.*, 14, 230 2015

TM cation migration – $\text{Li}_2\text{Ru}_{0.75}\text{Ti}_{0.25}\text{O}_3$

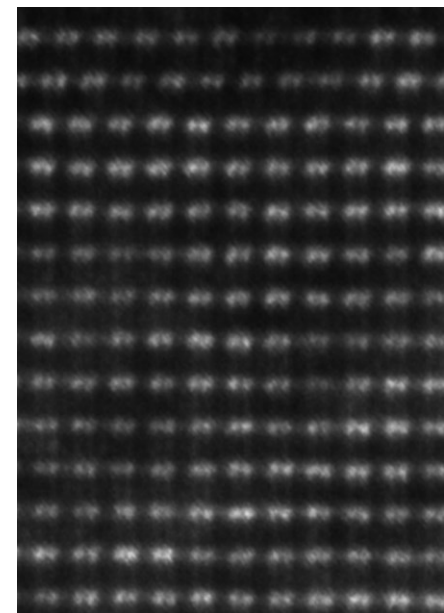
Pristine



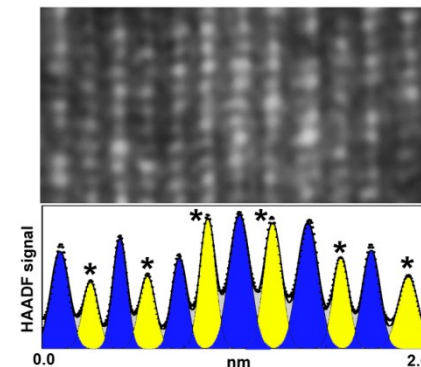
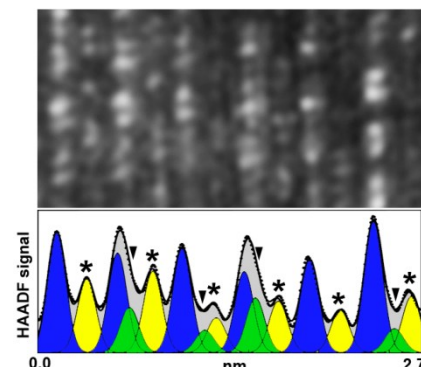
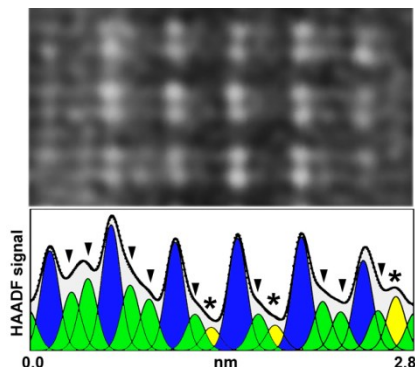
Charged to 4.6V



Discharged to 2V



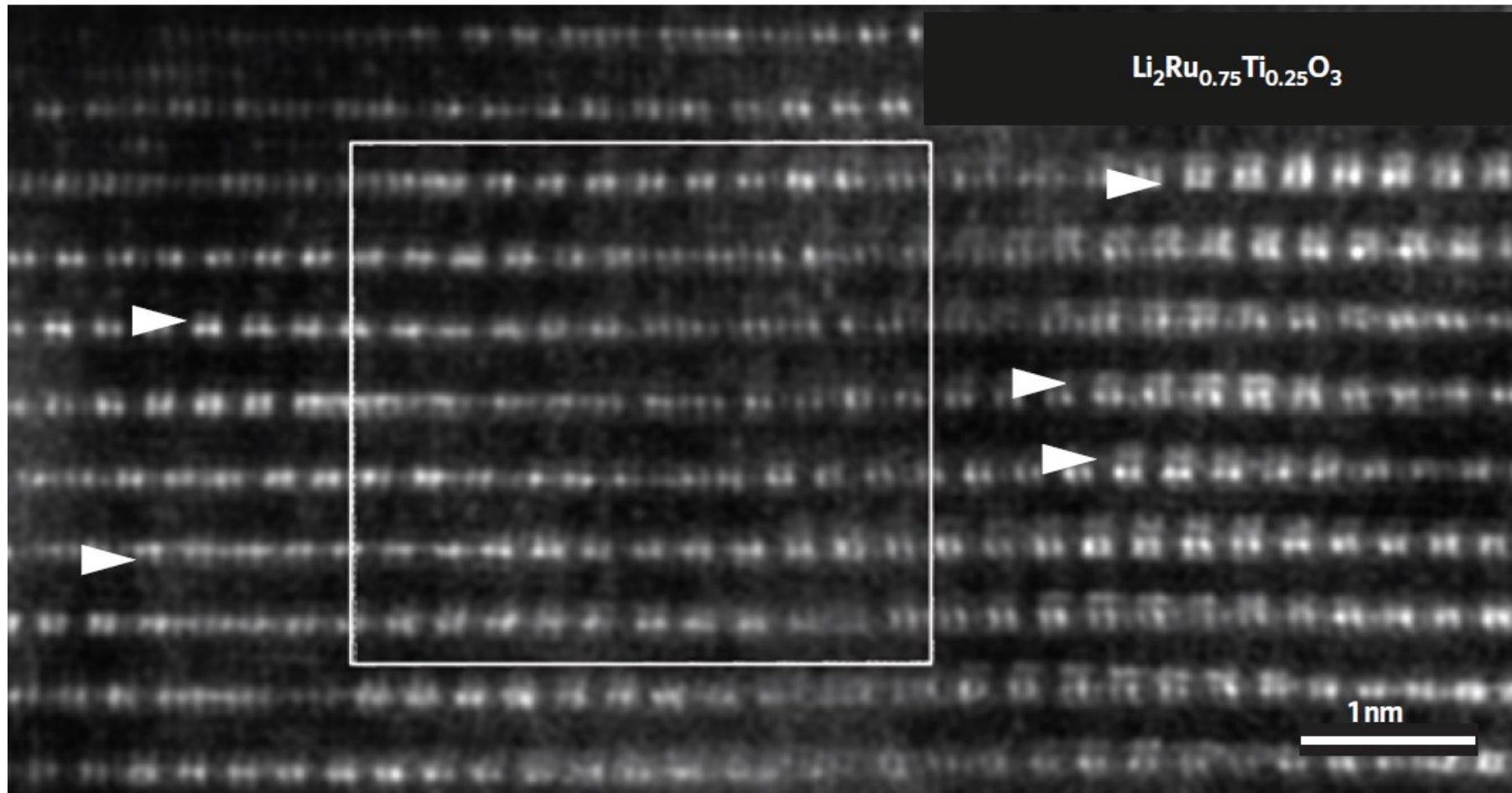
Structurally inhomogeneous charged state



- M_{oct}
- M_{Li}
- M_{tetr}

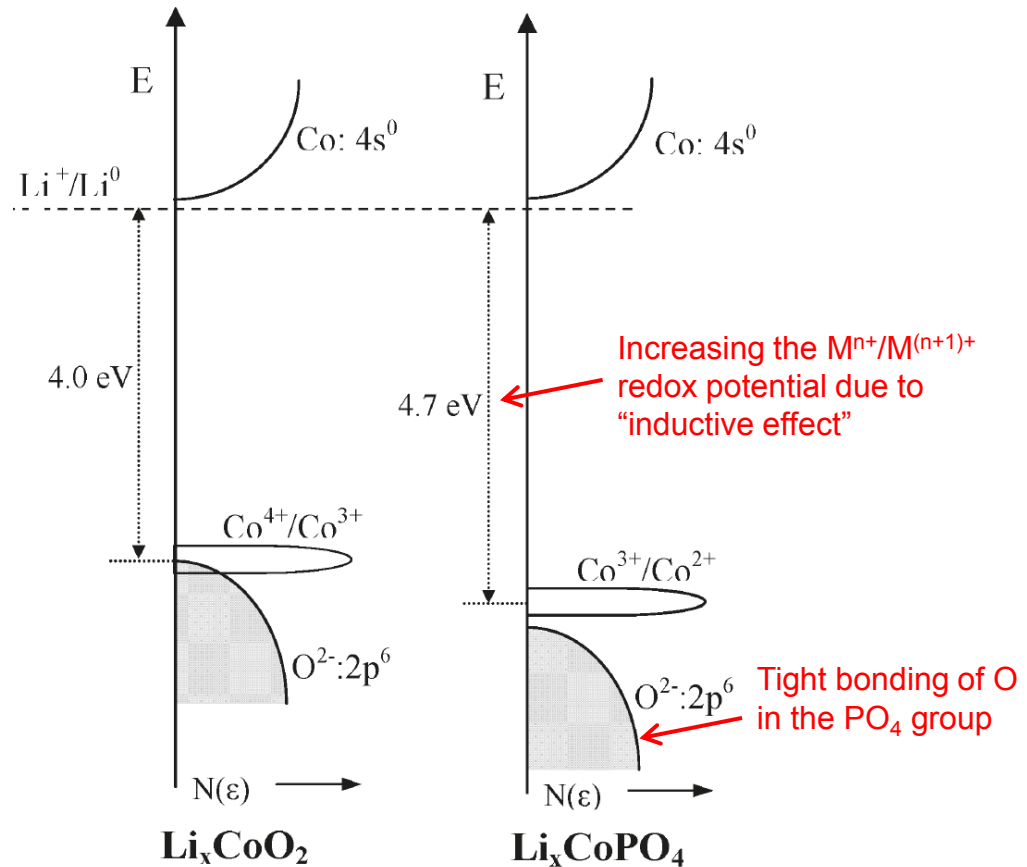
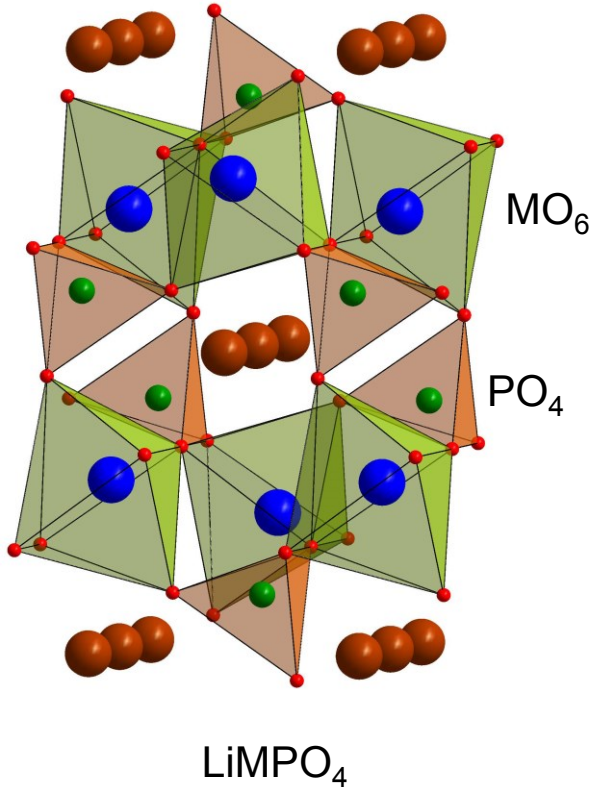
Sathiya, Abakumov, Foix,
Rousse, Ramesha, Saubanère,
Doublet, Vezin, Laisa, Prakash,
Gonbeau, Van Tendeloo,
Tarascon, *Nature Mater.*, 14, 230
2015

TM cation migration – $\text{Li}_2\text{Ru}_{0.75}\text{Ti}_{0.25}\text{O}_3$

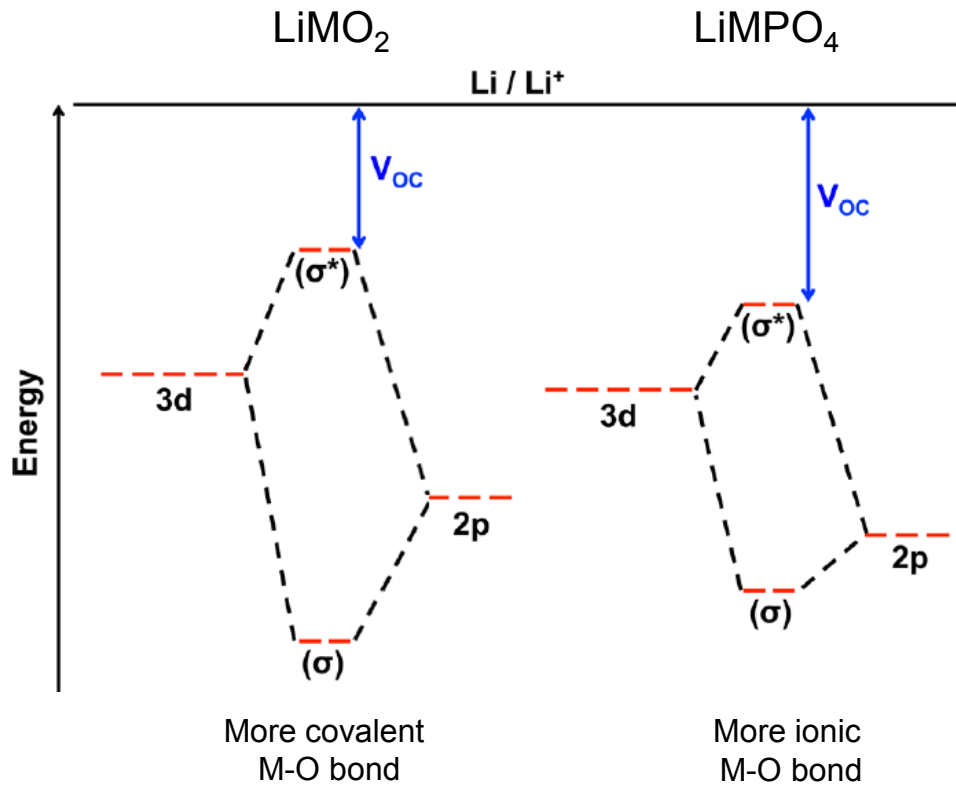


Discharged to 2V after 50 cycles: trapping of the TM cations at the tetrahedral interstices

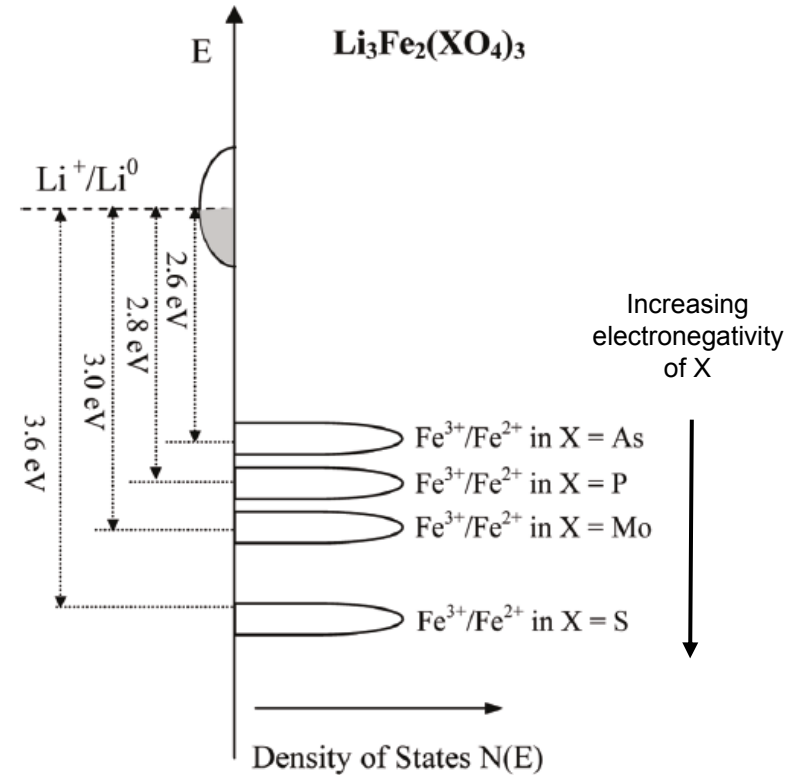
Polyanion cathode materials



Polyanion cathode materials



Tuning the $\text{M}^{n+}/\text{M}^{(n+1)+}$ redox potential through adjusting the M-O-X interactions



Tuning the $\text{M}^{n+}/\text{M}^{(n+1)+}$ redox potential through changing electronegativity of X

Cathodes with the olivine structure: LiFePO₄

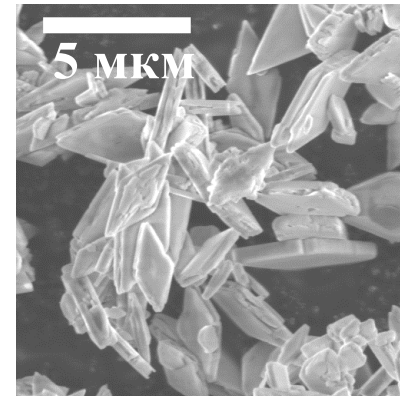
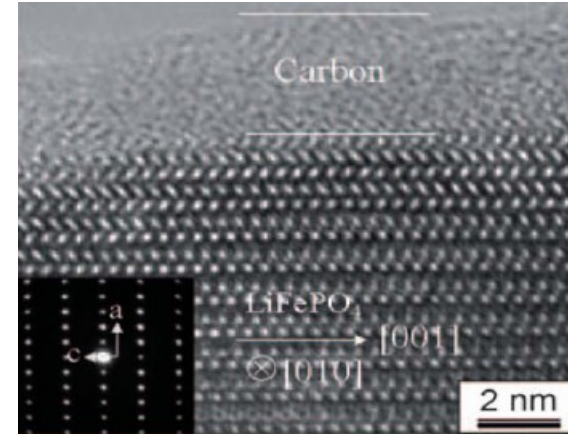
Capacity 170 mAh/g, voltage ~ 3.5 V

Pros:

- stability (3D structure + PO₄)
- LiFePO₄ \leftrightarrow FePO₄ + Li⁺ + e⁻
- environmentally benign
- low cost

Cons:

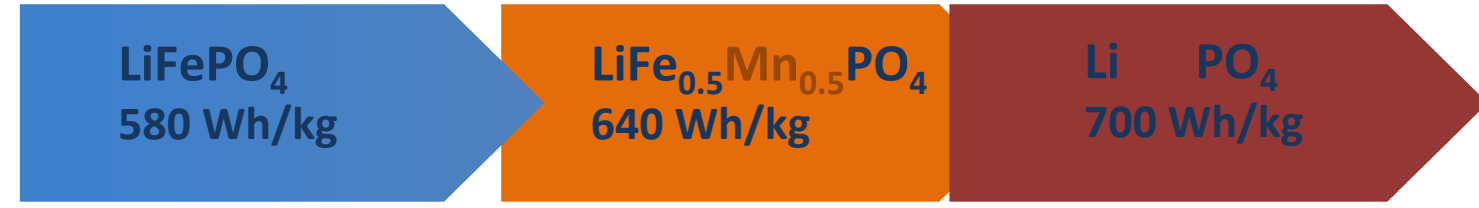
- low conductivity ~ 10⁻⁹ S/cm
- low Li⁺ diffusion coefficient ~10⁻¹⁵ cm²/s
- relatively low voltage



Solution:

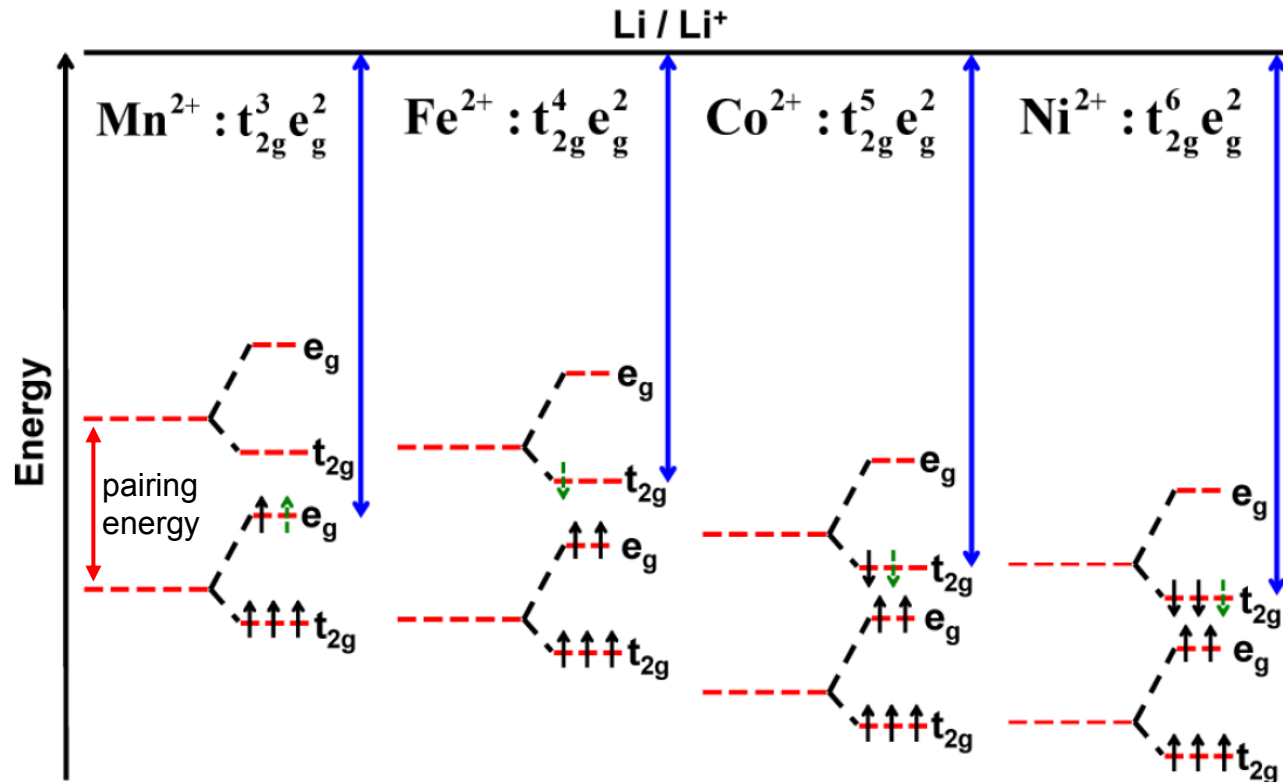
- conducting carbon coating
- nanosized particles
- optimized morphology
- platelets with 200 – 300 nm thickness along the fast diffusion direction
- high discharge current
(50% of discharge capacity / 1 min)

Cathodes with the olivine structure: $\text{Li}(\text{Mn},\text{Fe})\text{PO}_4$

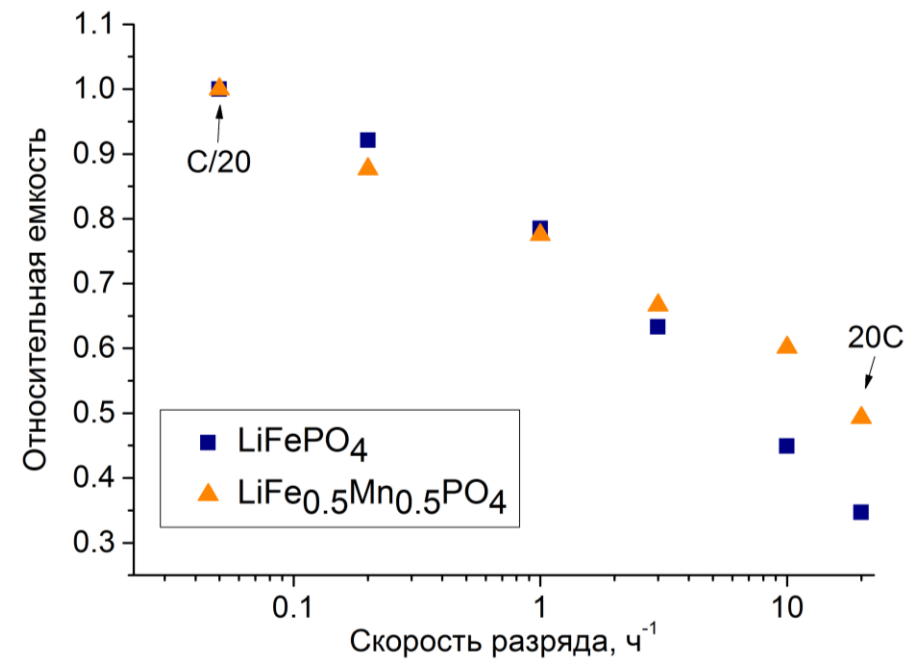
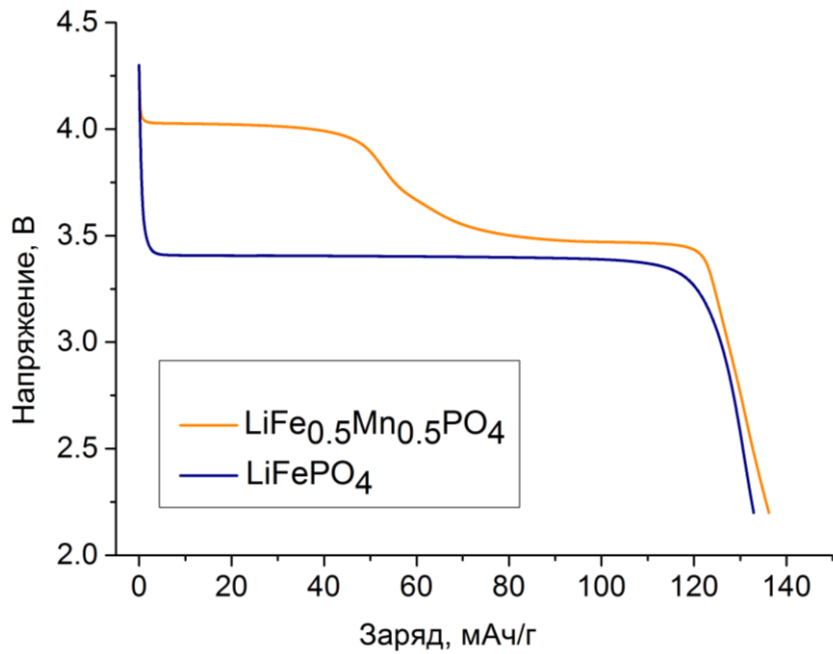


battery with $\approx 120 - 140$ Wh/kg

battery up to 150 - 175 Wh/kg



Cathodes with the olivine structure: $\text{Li}(\text{Mn},\text{Fe})\text{PO}_4$

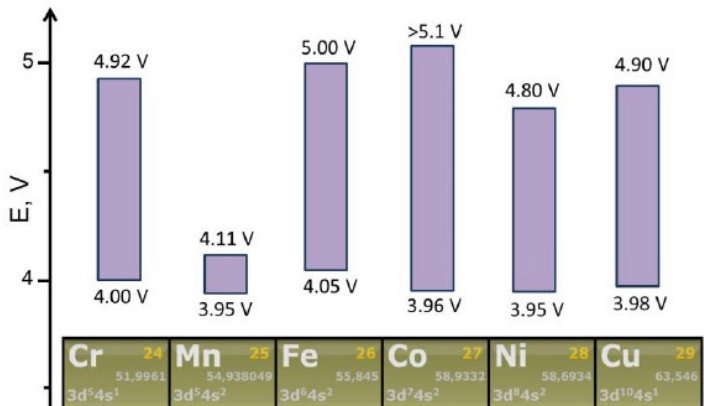
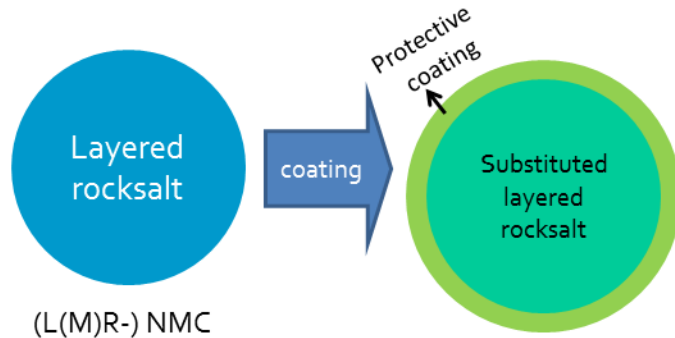


O.Drozhzhin, V.Sumanov, O.Karakulina, A.Abakumov, J.Hadermann, A.Baranov, K.Stevenson, E.Antipov,
J.Power Sources, 2015

Conclusions

Improvement of the cathode materials

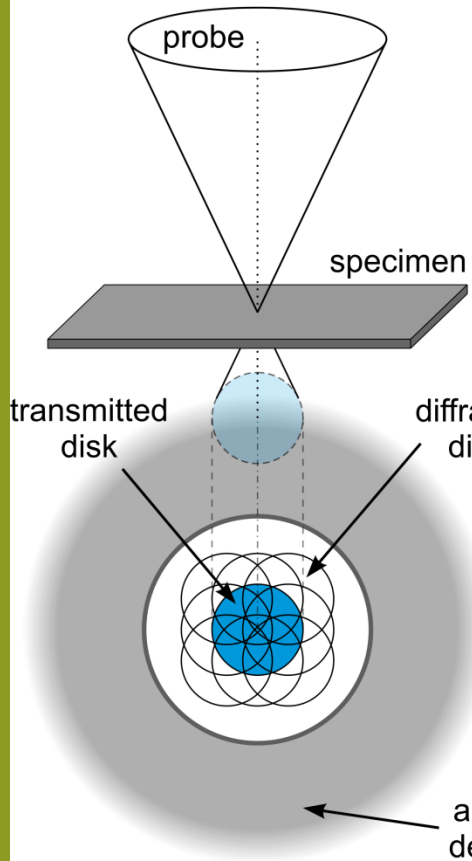
1. Chemical substitutions (metals with strong covalent bonding to O, cations blocking migration)
2. Protective coatings
3. Maximizing the energy density through tuning redox potential
4. Nanostructuring and functional coatings
5. New crystal structures and chemistries



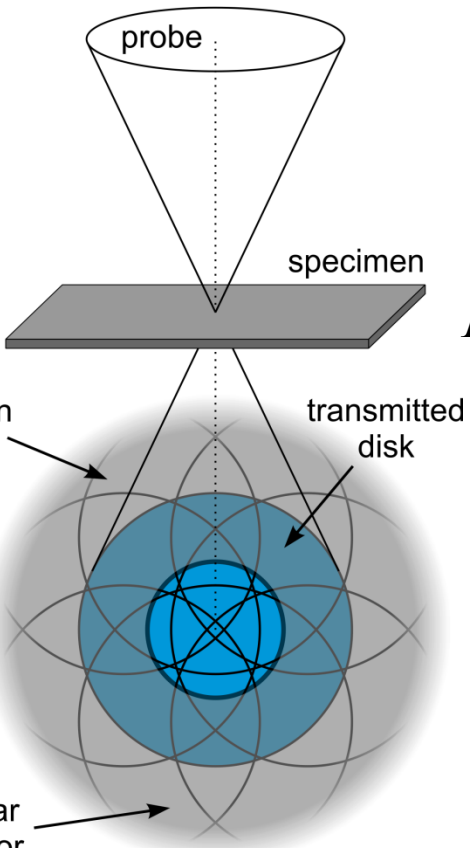
Stability windows for the $\text{LiMn}_{1.5}\text{M}_{0.5}\text{O}_4$ spinels

Thank you for your attention!

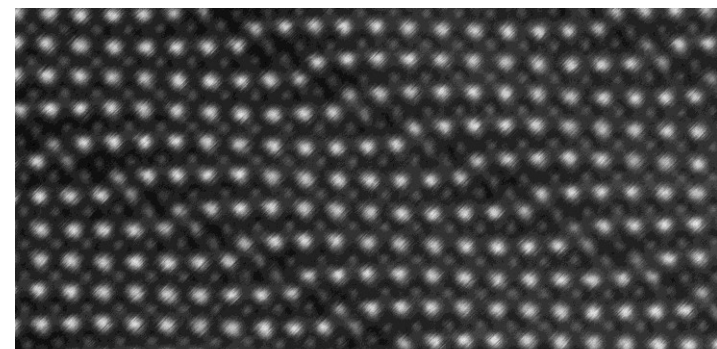
HAADF-STEM



ABF-STEM

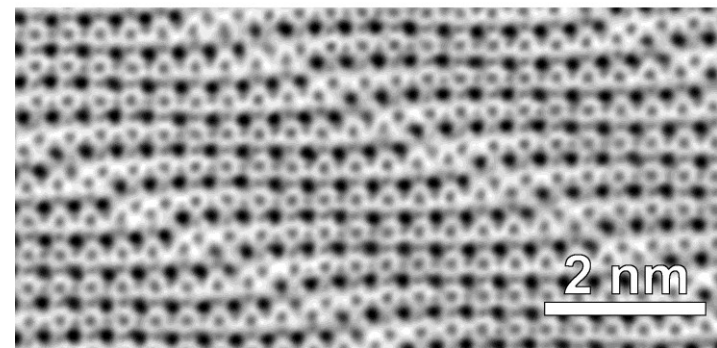


$$I \sim Z^2$$



HAADF-STEM

$$I \sim Z^{1/3}$$



ABF-STEM

HAADF-STEM – high angle annular dark field scanning transmission electron microscopy

ABF-STEM – annular bright field scanning transmission electron microscopy